J. Am. Soc. Mass Spectrom. (2017) 28:164–181
DOI: 10.1007/s13361-016-1512-z

RESEARCH ARTICLE

Where Does the Electron Go? Stable and Metastable Peptide Cation Radicals Formed by Electron Transfer

Robert Pepin,[1] Erik D. Layton,[1] Yang Liu,[1] Carlos Afonso,[2] František Tureček[1]

[1]Department of Chemistry, University of Washington, Bagley Hall, Box 351700, Seattle, WA 98195-1700, USA
[2]INSA Rouen, UNIROUEN, CNRS, COBRA, Normandie University, 76000, Rouen, France

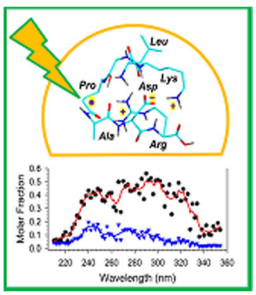

Abstract. Electron transfer to doubly and triply charged heptapeptide ions containing polar residues Arg, Lys, and Asp in combination with nonpolar Gly, Ala, and Pro or Leu generates stable and metastable charge-reduced ions, $(M + 2H)^{+\bullet}$, in addition to standard electron-transfer dissociation (ETD) fragment ions. The metastable $(M + 2H)^{+\bullet}$ ions spontaneously dissociate upon resonant ejection from the linear ion trap, giving irregularly shaped peaks with offset *m*/*z* values. The fractions of stable and metastable $(M + 2H)^{+\bullet}$ ions and their mass shifts depend on the presence of Pro-4 and Leu-4 residues in the peptides, with the Pro-4 sequences giving larger fractions of the stable ions while showing smaller mass shifts for the metastables. Conversion of the Asp and C-terminal carboxyl groups to methyl esters further lowers the charge-reduced ion stability. Collisional activation and photodissociation at 355 nm of mass-selected $(M + 2H)^{+\bullet}$ results in different dissociations that give sequence specific MS^3 spectra. With a single exception of charge-reduced $(LKGLADR + 2H)^{+\bullet}$, the MS^3 spectra do not produce ETD sequence fragments of the c and z type. Hence, these $(M + 2H)^{+\bullet}$ ions are covalent radicals, not ion–molecule complexes, undergoing dramatically different dissociations in the ground and excited electronic states. The increased stability of the Pro-4 containing $(M + 2H)^{+\bullet}$ ions is attributed to radicals formed by opening of the Pro ring and undergoing further stabilization by hydrogen atom migrations. UV–VIS photodissociation action spectroscopy and time-dependent density functional theory calculations are used in a case in point study of the stable $(LKGPADR + 2H)^{+\bullet}$ ion produced by ETD. In contrast to singly-reduced peptide ions, doubly reduced $(M + 3H)^{+}$ ions are stable only when formed from the Pro-4 precursors and show all characteristics of even electron ions regarding no photon absorption at 355 nm or ion-molecule reactions, and exhibiting proton driven collision induced dissociations.

Keywords: Metastable peptide ions, Electron transfer, Photodissociation, Action spectroscopy, Time-dependent DFT calculations

Received: 8 August 2016/Revised: 12 September 2016/Accepted: 15 September 2016/Published Online: 5 October 2016

Introduction

One-electron reduction and oxidation of proteins and peptides generates radicals that undergo a variety of reactions depending on the radical structure and environment. Radical-bearing groups in proteins have been associated with oxidation-prone residues (Tyr, Cys, Trp) and found to be of importance for the functioning of several redox enzymes, such as the iron-containing cytochrome *c* oxidase [1] and ribonucleotide reductase [2], iron-dependent pyruvate formate- lyase [3, 4], Cu-dependent galactose oxidase [5], and other metalloproteins [6, 7], as reviewed [8]. In contrast, nonspecific formation of radical sites in metal-free peptides and proteins has been observed upon electrochemical reduction [9, 10] and in various radical-induced chemical reactions [11–13].

A particularly efficient way of generating radical sites in proteins and peptides is by electron attachment to multiply protonated protein or peptide ions in the gas phase [14]. Cation radicals generated this way have quite unusual electronic structures and undergo extensive backbone dissociations resulting from electron attachment to amide groups that destabilizes the bonds between the amide nitrogens and C_α atoms at the adjacent residues [15]. The backbone cleavages have been used for efficient protein sequencing by electron capture dissociation

Electronic supplementary material The online version of this article (doi:10.1007/s13361-016-1512-z) contains supplementary material, which is available to authorized users.

Correspondence to: František Tureček; *e-mail:* turecek@chem.washington.edu

mass spectrometry [16, 17]. A related method utilizes electron transfer in ion-ion reactions of peptide polycations with anion-radicals, which is used for peptide sequencing by electron transfer dissociation (ETD) mass spectrometry [18]. Concomitant with dissociations, variable populations of cation radicals are observed that underwent charge reduction but did not dissociate. This phenomenon was observed in electron attachment to multiply charged proteins [19, 20], as well as in electron transfer to peptide ions [21]. The fraction of non-dissociating peptide cation radicals is known to decrease with the charge state of the peptide ion, with higher charge states giving less survivor peptide cation radicals [22]. When observed in ETD, this phenomenon is sometimes called ET-no-D [23] and is often viewed as an impediment to gas-phase peptide sequencing by ETD. The occurrence of non-dissociating peptide cation radicals in ETD mass spectra can be associated with the presence of particular amino acid residues, such as histidine [24, 25], that upon electron transfer undergo radical isomerizations forming stable cation-radical structures [26]. The fraction of non-dissociating peptide cation radicals can be substantially enhanced by performing electron transfer on multiply charged noncovalent peptide complexes with 18-crown-6-ether (CE), where the ligand coordination to the charged groups affects the electron attachment site [27, 28].

Non-dissociating peptide cation radicals produced by electron transfer have been studied by collision-induced dissociation (CID) [29, 30] and photodissociation [31], with the goal of achieving fragmentation to produce more sequence fragment ions [31, 32]. Alternatively, activation of the precursor ions by infrared radiation has been used to promote dissociation upon ETD (activated-ion ETD, AI-ETD) [33]. CID of charge-reduced ions from ETD have been reported to result in backbone dissociations that were accompanied by hydrogen transfer between the incipient fragments, yielding N-terminal $[c + H]^{+\bullet}$ cation radical fragments and C-terminal $[z + 2H]^{+}$ even-electron ions instead of the usual $[c + 2H]^{+}$ and $[z + H]^{+\bullet}$ fragment ions (Scheme 1).

For an all-inclusive nomenclature of peptide fragment ions see reference [34]. In contrast, CID and UV photodissociation (UVPD) of histidine-containing peptide cation radicals resulted in loss of H and side-chain cleavages, whereas no backbone dissociations were observed [35]. Non-dissociating charge-reduced cation radicals that were produced by electron capture in +4 and +3 charge states of the disulfide bridges containing peptide lacticin were found to eliminate SH radicals upon CID, but very few low intensity backbone fragment ions were observed [36]. Charge-reduced peptide ions [21, 37] and ubiquitin 6+ and 5+ ions [38] were studied by ion-molecule reactions and found to undergo radical induced addition of up to three O_2 molecules. However, CID of the O_2 adducts resulted in loss of OH and OOH that were not indicative of the peptide radical structure.

Most of the previous studies have been focused on analyzing dissociation products from randomly selected charge-reduced peptides, whereas the structure and electronic properties of the pertinent cation radicals have been addressed in only a few cases [35]. Here, we use the recently described rationally designed peptide ions of the [R, L, G, A, D, K, X] type [39] (X = Pro or Leu) to investigate the structures and properties of cation radicals resulting from attachment of one or two electrons. We employ CID and ion-molecule reactions to investigate the ground-state chemistry of the peptide cation radicals. Near-UV photodissociation is employed to specifically target the radical chromophores [35, 40, 41] and investigate their excited state chemistry. UV–VIS photodissociation action spectroscopy [42, 43] along with density functional theory electron structure calculations are used to characterize the diverse radical structures [44, 45] resulting from electron attachment to these peptide ions. We wish to show that even minor sequence and residue variations in peptides have a large effect on the chemistry of cation radicals produced by electron transfer.

Experimental

Materials

Standard synthetic heptapeptides LKGPADR, LRGPADK, KLGPADR, RLGPADK were acquired from United Biosystems (Cabin John, MD, USA, 95% purity or better) and used without further purification. Heptapeptides LKGLADR, LRGLADK, KLGLADR, RLGLADK were purchased from GenScript (Piscataway, NJ, USA, 95% purity or better). Solvents and methylation reagents were purchased from Sigma Aldrich (St. Louis, MO, USA) and used as received. Heptapeptide dimethyl esters were prepared as described previously [39].

Methods

ETD-MS^n spectra were measured on an LTQ-XL-ETD linear ion trap (ThermoElectron Fisher, San Jose, CA, USA) equipped with an auxiliary negative chemical ionization (NCI) ion source for the production of fluoranthene anions

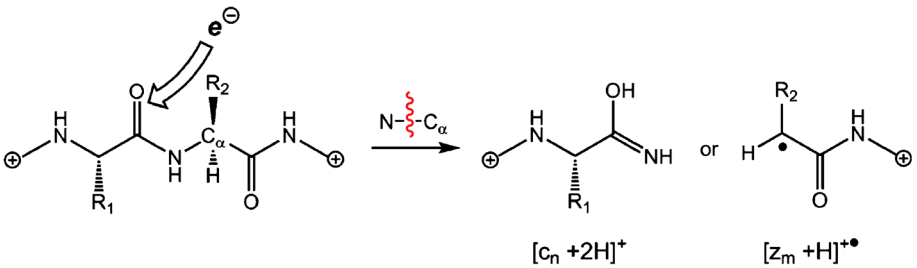

Scheme 1. Backbone dissociations in ETD

with nitrogen as a source moderator gas. Another set of ETD-MS^n spectra were acquired on an Esquire HCT Ultra ion trap (Bruker Daltonics, Bremen, Germany) equipped with an auxiliary negative chemical ionization ion source (methane as moderator gas, −4 V NCI source bias) to produce fluoranthene anions [46]. Doubly and triply charged peptide ions were produced by electrospray ionization from 5–10 microM solutions in methanol–water-acetic acid, 50:50:0.5, stored in the ion trap and allowed to react with fluoranthene anions for 100 or 200 ms for the triply and doubly charged ions, respectively. The standard scan rate was 8100 and 16,666 *m/z* units/s on the Bruker HCT-ultra-ETD and LTQ-XL ion traps, respectively. A slow ("zoom") scan rate of 1100 *m/z* units/s was used to obtain mass-resolved peptide cation-radical peak profiles on the LTQ for metastable peak analysis. UV photodissociation spectra at 355 nm were obtained with an EKSPLA NL 301 HT (Altos Photonics, Bozeman, MT, USA) Nd-YAG laser operating at 20 Hz frequency with a 3–6 ns pulse width. The laser is equipped with a third harmonics frequency generator producing a single 355 nm wavelength at 120 mJ/pulse peak power. The typical laser power used in the photodissociation experiments was 15–20 mJ/pulse. UV–VIS photodissociation action spectra of charge-reduced and mass-selected peptide ions were measured on the LTQ-XL as described previously [41]. Briefly, the laser beam was produced by an Nd-YAG EKSPLA NL301G laser (Altos Photonics) operating at 20 Hz frequency with a 3–6 ns pulse width feeding a PG142C third harmonic generator and optical parametric oscillator coupled with an optional second harmonic generator (SH) to provide 0.79–2.06 mJ pulse peak power at wavelengths tunable between 210 and 409 nm. High-resolution ETD and ETD/CID mass spectra were measured on an LTQ-Orbitrap Velos instrument (ThermoElectron Fisher, San Jose, CA, USA) at a resolving power set to 100,000.

Calculations

Standard ab initio and density functional theory (DFT) calculations were performed to obtain ion structures, harmonic frequencies, and energies. Geometries were optimized with the hybrid functional ωB97X-D [47] and the 6-31+G(d,p) basis set. All calculations of open shell species were carried out with the spin-unrestricted formalism. Excited-state energies and oscillator strength were calculated with time-dependent DFT (TD-DFT) [48] using ωB97X-D and the 6-31+G(d,p) and 6-311++G(2d,p) basis sets. This combination of TD-DFT and basis sets has been previously benchmarked for excited-state calculations of peptide radical groups [49]. All calculations were performed with the Gaussian 09 suite of programs [50].

Note on Nomenclature

Fragment ions produced by dissociations of peptide cation radicals often differ in the number hydrogen atoms. This feature and the ion charge and electron parity are conveniently expressed by the all-inclusive nomenclature described recently that uses the hydrogen count in neutral peptide fragments as reference [34]. The conversion from the common Roepstorff-Fohlman-Biemann nomenclature [51, 52] is as follows for the present fragment ions: $\boldsymbol{z_n} = [z_n + H]^{+\bullet}$, $\boldsymbol{z_n} + 1 = [z_n + 2H]^+$, $\boldsymbol{c_m} = [c_m + 2H]^+$, $\boldsymbol{c_m} - 1 = [c_m + H]^{+\bullet}$, $\boldsymbol{a_k} = [a_k]^+$, $\boldsymbol{b_r} = [b_r]^+$, $\boldsymbol{x_l} = [x_l + H]^{+\bullet}$, $\boldsymbol{y_v} = [y_v + 2H]^+$

Results

Electron transfer dissociation of the heptapeptide ions and their dimethyl esters generated standard ETD mass spectra showing dissociations of N–C_α bonds and forming C-terminal fragment ions of the ***z*** type and *N*-terminal ***c*** type ions. Selected aspects of the dissociations are briefly described here. Backbone cleavage was observed in all positions except the *N*-terminal site of the Pro residue [14, 53]. For the doubly charged ions, the Arg-C-terminated peptides produced predominantly C-terminal (***z***-type) fragment ions that were complemented by abundant $[c_6 + 2H]^+$ and $[y_5 + 2H]^+$ fragment ions due to the respective Asp-Arg N–C_α and (Leu,Lys)-Gly CO–NH backbone cleavages. This is illustrated by the ETD spectrum of $(LKG\boldsymbol{P}ADR + 2H)^{2+}$ (Figure 1a), where the backbone fragment ions total 25% of the charge-reduced ion intensity. ETD spectra of the +2 and +3 charge states of the other peptides and their dimethyl esters are presented in Supplementary Figures S1–S11 (in Electronic Supplemental Information). Regarding ETD of the doubly charged ions, the $[y_5 + 2H]^+$ ion formation was suppressed in ETD of the doubly charged dimethylesters with the exception of LKG***L***ADR-di-Me ester (Supplementary Figure S9a). The effect of Asp on promoting cleavage of an adjacent amide bond in gas-phase ions is well known [54–56]. However, long-range Asp effects as well as those of carboxyl esterification have not been studied.

The doubly charged Lys-C-terminated ions uniformly produced Arg-containing *N*-terminal fragment ions of the ***c*** series that were accompanied by $[a_5 + H]^{+\bullet}$ and $[a_6 + H]^{+\bullet}$ fragment ions, whereas most ***z***-type ions were either absent or weak. The preponderance of Arg-containing fragment ions in the ETD spectra is likely due to the Arg superior basicity, as the fragments compete for the single remaining proton in intermediate complexes formed by N–C_α bond cleavage [53, 57]. Interestingly, the $[z_6 + H]^{+\bullet}$ fragment ion relative intensity was substantially enhanced in the ETD spectra of doubly charged LRG***P***ADK and LRG***L***ADK dimethyl esters (Supplementary Figures S9–S11), indicating specific backbone cleavage between the Leu and Arg residues. The presence of the $[a_5 + H]^{+\bullet}$ and $[a_6 + H]^{+\bullet}$ fragment ions indicates homolytic cleavage of the backbone C_α–CO bonds in the Arg-*N*-terminated peptide ions. This fragmentation is observed across this ion series with slightly enhanced $[a_5 + H]^{+\bullet}$ and $[a_6 + H]^{+\bullet}$ ion relative intensities in the ETD spectra of the dimethyl esters. Formation of $[a_n + H]^{+\bullet}$ fragment ions has also been reported for electron capture dissociation of doubly charged arginine-*N*-terminated peptide ions but not their amides [58]. The nature of this effect and its relationship to the peptide ion structure are not well understood.

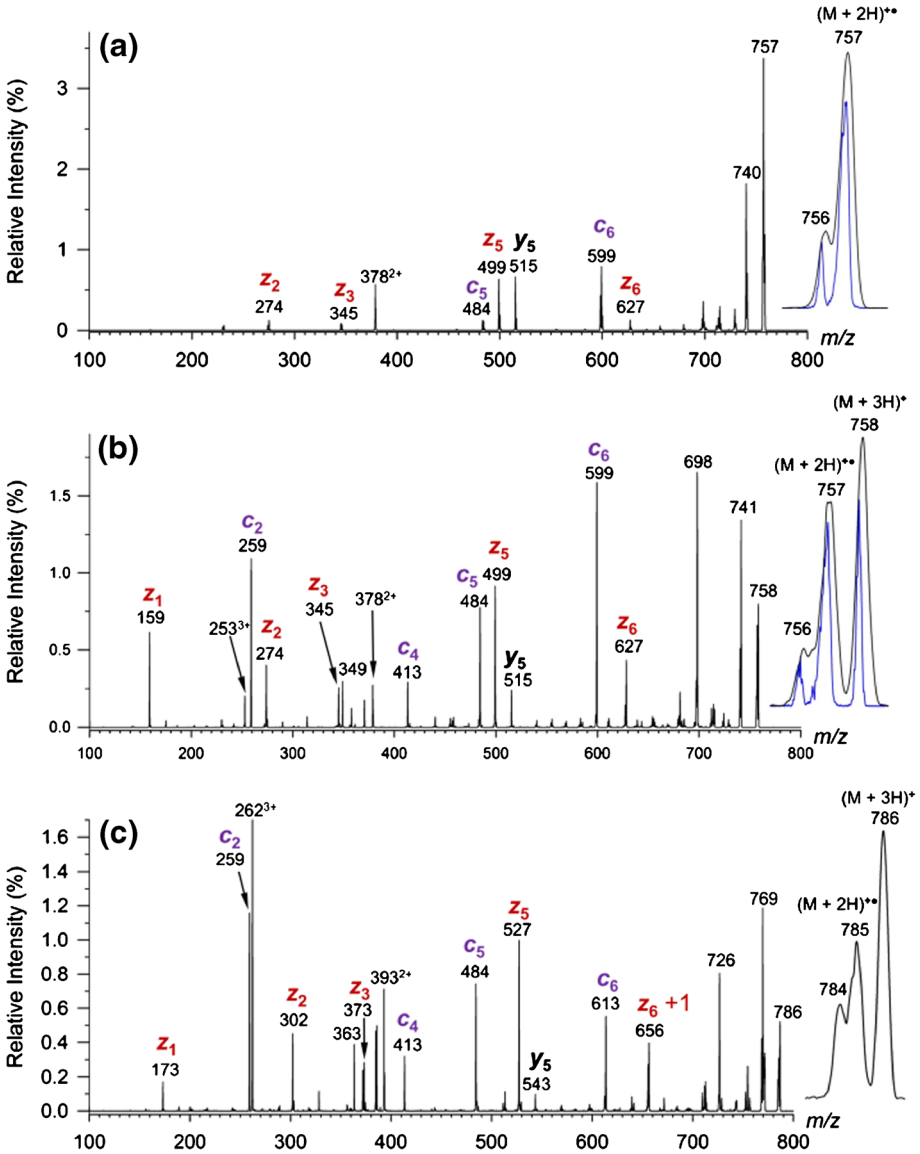

Figure 1. ETD mass spectra of (**a**) (LKG***P***ADR + 2H)$^{2+}$; (**b**) (LKG***P***ADR + 3H)$^{3+}$; (**c**) (LKG***P***AD(OCH$_3$)R(OCH$_3$) + 3H)$^{3+}$. Insets show the peak profiles for charge-reduced ions from regular (black) and zoom (blue) scans

Finally for this section, the ETD mass spectra of the triply charged ions showed extensive backbone cleavages breaking most of the N–C$_\alpha$ bonds and forming ***c*** and ***z*** type ions. Fragment ion assignments were facilitated by mass shifts (or absence thereof) because of Pro-Leu substitutions and C-terminal and Asp carboxyl methylation in the peptides, as shown in Figure 1b, c and Supplementary Figures S1–S11.

Metastable Peak Analysis

A conspicuous feature of the ETD spectra of the doubly and triply charged ions was the presence of charge-reduced but non-dissociating species (Figure 1a–c). For (LKGPADR + 2H)$^{2+}$ shown in Figure 1a, the (LKGPADR + 2H)$^{+\bullet}$ ion represented 48% of the total ETD ion intensity. These ions showed different peak shapes and relative intensities depending on the charge state of the peptide ion being reduced, the amino acid sequence, and derivatization to dimethyl esters. Figure 2 illustrates the peak profiles of charge-reduced ions from (KLG***X***ADR + 2H)$^{2+}$. The hydrogen-rich (M + 2H)$^{+\bullet}$ cation radicals showed composite shapes consisting of narrow components with a regular mass defect and full width at half maximum, which overlapped with broader, irregularly shaped peaks that were shifted 0.2–0.4 *m/z* units to lower values. To deconvolute the contribution of regular (M + 2H)$^{+\bullet}$ ions, the peaks of deprotonated singly charged (M + H)$^+$ ions were used as reference, showing regular Gaussian-line profiles with mass defects of +0.45 to +0.5 *m/z* units and full widths at half maximum (FWHM) of 0.18–0.20 *m/z* units. These mass defects and peak widths were also typical of fragment ions in this mass range [e.g., the abundant (MH − NH$_3$)$^{+\bullet}$ ions]. The regularly shaped peaks were deconvoluted by Gaussian profile fitting in the zoom spectra, and the integrated relative intensities of both types of ions and the mass shifts for the metastables are summarized in Table 1.

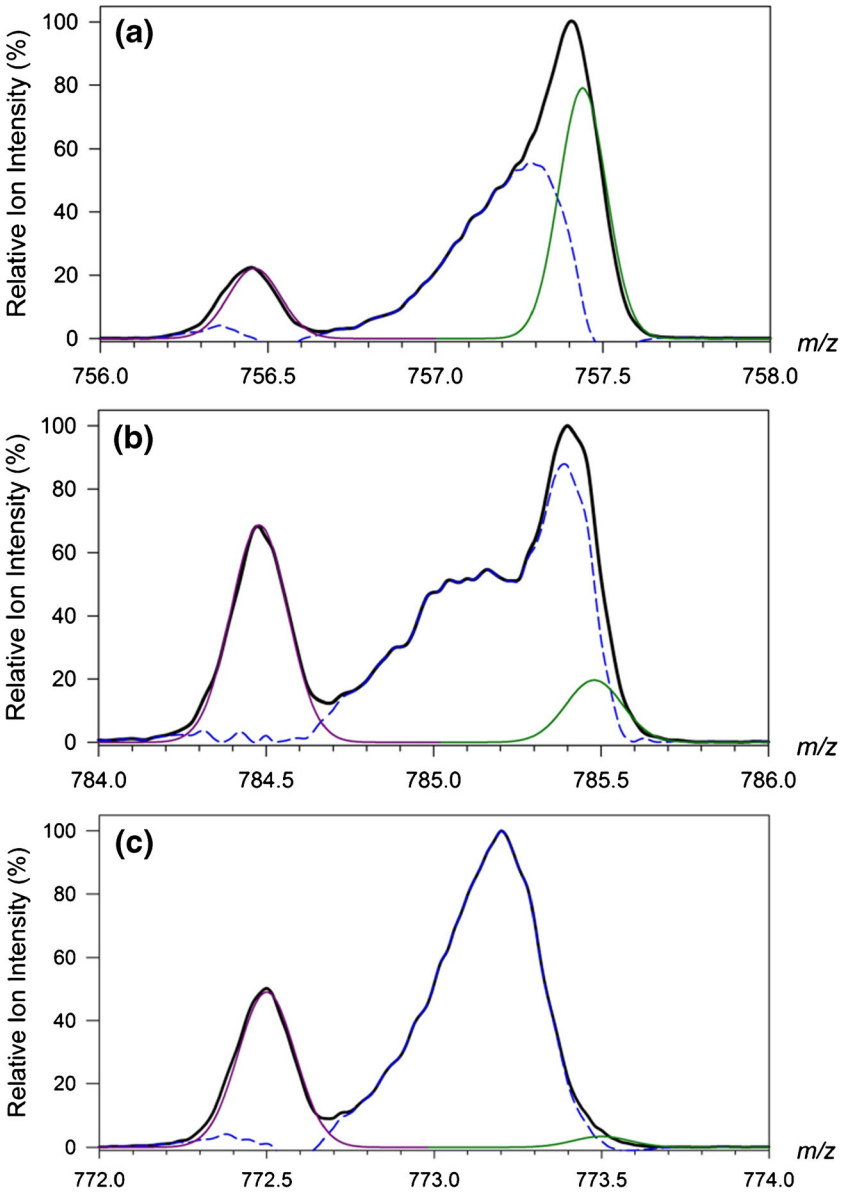

Figure 2. Peak profiles for charge-reduced ions from (**a**) $(KLG\boldsymbol{P}ADR + 2H)^{2+}$, (**b**) $(KLG\boldsymbol{P}AD(OCH_3)R(OCH_3) + 2H)^{2+}$, and (**c**) $(KLG\boldsymbol{L}ADR + 2H)^{2+}$. Black: experimental peak profiles from zoom scans; green: deconvoluted peak profiles of stable $(M + 2H)^{+\bullet}$; magenta: deconvoluted peak profiles of stable $(M + H)^{+}$; blue: deconvoluted peak profiles of metastable $(M + 2H)^{+\bullet}$

The irregular peak shapes are indicative of metastable ions that undergo dissociations in the early stages of ejection from the ion trap [29, 59]. For the LTQ-XL in particular, mass-selective ion ejection is accomplished by resonant excitation at a fixed q value of 0.88 ($\beta_x \approx 0.9$) [60]. This resonant excitation, also called 'axial modulation', accomplishes ejection of the ions before the natural ejection point of the ion trap at $q = 0.908$ [61]. As the q value of the ion is increased during the mass scan, the amplitude and radial velocity of the ion motion increases to trigger vibrational excitation by collisions with the buffer gas. This can cause dissociation of weakly bound ions, and the ensuing fragment ions of lower m/z that have higher q values are ejected before the parent ion. Irregular peak shapes have been previously observed for charge-reduced peptide ions [35], fragment ions of the ***x***-type [62], as well as for noncovalent peptide [41] and lipid complexes [63].

The shape and composition of the peaks of charge-reduced peptide ions differed depending on the peptide sequence and charge state (Table 1). Regarding ETD of doubly charged ions, the proline peptides showed 30%–50% fractions of regularly shaped and positioned peaks for the charge-reduced cation radicals, but also substantial (50%–70%) fractions of metastable species. This is illustrated by the peak profiles for $(KLG\boldsymbol{P}ADR + 2H)^{+\bullet}$ (Figure 2a); those for the other peptides are shown in Supplementary Figures S12–S16. These metastable peaks showed only small mass shifts (−0.04 to −0.06 m/z units), indicating that they dissociated at translational excitations close to the ion ejection point. The proportion of

Table 1. Metastable Peaks of Charge-Reduced $(M + 2H)^{+\bullet}$ Peptide Cation Radicals

Precursor ion	Metastable fraction		Mass shift (m/z)[a]	
	X= Pro	X=Leu	X=Pro	X=Leu
$(LKGXADR + 3H)^{3+}$	75	98	−0.18	−0.30
$(LKGXADR + 2H)^{2+}$	47	97	−0.04	−0.22
$(LKGXADR(OCH_3)_2 + 3H)^{3+}$	81	99	−0.10	−0.38
$(LKGXADR(OCH_3)_2 + 3H)^{2+}$	77	99	−0.28	−0.41
$(KLGXADR + 3H)^{3+}$	74	98	−0.08	−0.36
$(KLGXADR + 2H)^{2+}$	60	85	−0.04	−0.30
$(KLGXADR(OCH_3)_2 + 3H)^{3+}$	71	97	−0.10	−0.48
$(KLGXADR(OCH_3)_2 + 3H)^{2+}$	91	97	−0.08	−0.42
$(LRGXADK + 3H)^{3+}$	76	97	−0.08	−0.37
$(LRGXADK + 2H)^{2+}$	69	99	−0.06	−0.35
$(LRGXADK(OCH_3)_2 + 3H)^{3+}$	84	99	−0.08	−0.42
$(LRGXADK(OCH_3)_2 + 3H)^{2+}$	88	99	−0.12	−0.38
$(RLGXADK + 3H)^{3+}$	75	80	−0.10	−0.30
$(RLGXADK + 3H)^{2+}$	64	84	−0.04	−0.38
$(RLGXADK(OCH_3)_2 + 3H)^{3+}$	86	95	−0.10	−0.44
$(RLGXADK(OCH_3)_2 + 3H)^{2+}$	82	98	−0.08	−0.44

[a]Relative to the stable ion m/z values

metastables increased to 77%–91% for the dimethyl esters derived from the proline peptides, and also the mass defects increased, indicating lower stability of these cation radicals (Figure 2b).

The metastable peak in Figure 2b appears to be bimodal, composed of a less stable fraction showing a large (−0.4 m/z unit) shift, and a more stable fraction showing a small mass shift (−0.1). In a stark contrast, the homologous leucine peptides showed dominant fractions (84%–97%) of metastable charge-reduced cation radicals that had large mass shifts (−0.22 to −0.38 m/z units, (Figure 2c), which further increased for metastable cation radicals from the related methyl esters (Table 1).

Double electron transfer to the triply charged peptide ions showed another strong effect of the survivor singly charged ion peak shape, position, and relative intensity. All triply charged peptide ions of the Pro series, including the methyl esters, produced stable $(M + 3H)^+$ ions of regular shape and m/z position, as illustrated by the spectrum of $(KLGPADR + 3H)^{3+}$ in Figure 3a. In contrast to the proline peptides, triply charged peptide ions of the Leu series did not produce metastable or stable $(M + 3H)^+$ ions (Figure 3b) regardless of their sequence or carboxyl methylation.

The $(M + 2H)^{+\bullet}$ ions produced by charge reduction of triply charged ions showed composite peak shapes that were analogous to those observed for the same species generated by charge reduction of doubly charged ions. The $(M + 2H)^{+\bullet}$ ions can be formed by two pathways that differ in the sequence of electron attachment and hydrogen loss: (1) $(M + 3H)^{3+} + e \rightarrow (M + 3H)^{2+\bullet} \rightarrow (M + 2H)^{2+} + H^{\bullet}$; $(M + 2H)^{2+} + e \rightarrow (M + 2H)^{+\bullet}$, or (2) $(M + 3H)^{3+} + 2e \rightarrow (M + 3H)^{+} \rightarrow (M + 2H)^{+\bullet} + H^{\bullet}$. The relative intensities of the metastable fractions of the $(M + 2H)^{+\bullet}$ ions from triply charged carboxyl-terminated peptide ions were similar to those from doubly charged precursors (Table 1), indicating their formation by pathway (1) as the major process. Of note is that charge-reduction of triply charged peptide ions with *N*-terminal Leu residues showed greater relative intensities of $(M + 2H)^{+\bullet}$ ions than did those with *N*-terminal Lys or Arg residues (Supplementary Figures S17a, b–S19a, b).

CID Characterization of Charge-Reduced Peptide Cation Radicals

The charge-reduced peptide ions were selected by mass and further characterized by CID and UVPD-MS^3 spectra. The mass-selected ions showed regular peak profiles upon mass scans, indicating that only the stable fractions survived ion isolation to be further investigated by MS^n measurements. For peptide sequences giving very low stable fractions of charge-reduced ions, the isolated ion intensity was insufficient for obtaining good quality MS^3 spectra. CID of $(LKGPADR + 2H)^{+\bullet}$, originating from electron transfer to the doubly charged precursor ion, triggered a single dominant dissociation by loss of a C_3H_7 radical (Figure 4a). The neutral loss assignment was corroborated by accurate mass measurements (Δm = 43.0558 Da, C_3H_7 requires 43.0548 Da). A dominant loss of C_3H_7 was also observed on CID of the $(M + 2H)^{+\bullet}$ ion from double electron transfer to $(LKGPADR + 3H)^{3+}$, which gave a spectrum (Supplementary Figure S20a) that was identical to that in Figure 4a. A very similar dissociation pattern, dominated by loss of C_3H_7, was also found for charge-reduced LKGPADR-dimethyl ester (Supplementary Figure S20b, c). In the case of low energy CID of peptide cation radicals, loss of C_3H_7 is characteristic of the Leu residue [64, 65] and is particularly facilitated by the formation of a Leu-C_α radical that triggers β-fission of the C_β–C_γ bond in the alkyl side chain [64, 66].

In contrast, CID of the Leu analog $(LKGLADR + 2H)^{+\bullet}$ resulted in backbone dissociations between the Ala-Asp, Leu-Ala, and Asp-Arg residues forming the respective $[z_2 + 2H]^+$, $[z_3 + 2H]^+$, $[c_5 + H]^{+\bullet}$, and $[c_6 + H]^{+\bullet}$ fragment ions, whereas the loss of C_3H_7 was nearly absent (Figure 4b). The formation of these backbone fragment ions was associated with hydrogen and proton atom migrations between the incipient $[z_n + H]^{+\bullet}$ and $[c_m + H]$ fragments in ion–molecule complexes formed by N–C_α bond cleavages, indicating that the charge-reduced $(LKGLADR + 2H)^{+\bullet}$ ions consisted of a mixture of isomeric ion–molecule complexes. We note that LKGLADR was the only sequence among those we studied that showed this fragmentation pattern, which is analogous to those previously observed for ET-CAD of other peptide ions [29, 30]. This further underscores the effects of sequence on the charged-reduced peptide ion chemistry.

Switching the Leu and Lys positions as in KLGPADR and KLGLADR resulted in major changes in the CID spectra of the charge-reduced ions. CID of $(KLGPADR + 2H)^{+\bullet}$ led to a minor loss of C_3H_7, whereas the main dissociation was a loss of a 58 Da neutral fragment (Figure 4c, Supplementary Figure S21a). The charge-reduced ion from KLGPADR-dimethyl ester showed an entirely analogous CID spectrum, regardless of the precursor ion charge, indicating that the 58 Da neutral fragment was not $C_2H_2O_2$ originating from the Asp residue

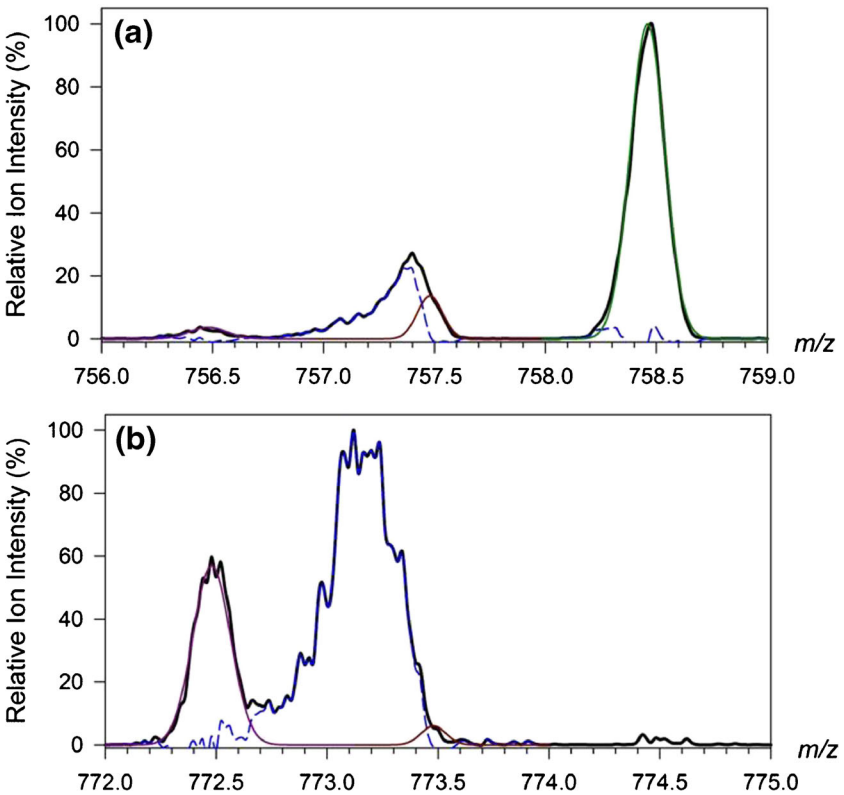

Figure 3. Peak profiles of charge-reduced ions from (**a**) (KLG***P***ADR + 3H)$^{3+}$ and (**b**) (KLG***L***ADR + 3H)$^{3+}$. Black: experimental peak profiles from zoom scans; green: deconvoluted peak profiles of stable (M + 3H)$^{+}$; magenta: deconvoluted peak profiles of stable (M + 2H)$^{+\bullet}$; blue: deconvoluted peak profiles of metastable (M + 2H)$^{+\bullet}$; dark red: deconvoluted peak profiles of stable (M + H)$^{+}$

(Supplementary Figure S21b, c). We assign the 58 Da fragment to a $H_2NCH_2CH_2CH_2^{\bullet}$ radical from the Lys side chain where its loss can be triggered by β-fission of the C_β–C_γ bond in a Lys-C_α radical intermediate.

In a yet another contrasting result, CID of (KLG***L***ADR + 2H)$^{+\bullet}$ resulted in a dominant loss of water (Figure 4d, Supplementary Figure S22a). The charge-reduced ion from KLG-***L***ADR-dimethyl ester showed an analogous loss of methanol, indicating that these molecules originated from the respective Asp or Arg carboxyl and methoxycarbonyl groups (Supplementary Figure S22b). Radical bond cleavage in (KLG***L***ADR + 2H)$^{+\bullet}$ resulted in the formation of the *m/z* 599 fragment ion by loss of 174 Da that we assign to an elimination of a neutral Arg molecule (Figure 4d). A homologous $[b_6 + H]^{+\bullet}$ fragment (*m/z* 613) is very minor in the CID spectrum of the dimethyl ester (Supplementary Figure S22b), which is consistent with the higher basicity of Arg methyl ester and proton retention in this small fragment, the *m/z* of which is below the low-mass cutoff of the ion trap and, therefore, the ion does not appear in the spectrum.

Charge-reduced peptide ions with the Arg residue close to the *N*-terminus showed different fragmentations in CID. Starting with (LRG***P***ADK + 2H)$^{+\bullet}$, CID triggered loss of C_3H_7 followed by a facile loss of ammonia to give the most abundant fragment ion at *m/z* 697 (Figure 5a). The identity of the neutral molecules was established by accurate mass measurements. Competing with this pathway was a dissociation by loss of $C_6H_{13}N_2O_2$, which is a (Lys − H)$^{\bullet}$ radical, forming a $[b_6 + 2H]^{+}$ fragment ion at *m/z* 612. Also seen is a loss of $C_7H_{13}N_2O_3$ forming the $[a_6 + 2H]^{+}$ fragment ion at *m/z* 584.

CID of the charge-reduced LRG***P***ADK dimethyl ester shows a dominant loss of C_3H_7 which, however, is followed by only a very minor loss of ammonia (Supplementary Figure S23a, b). The $[b_6 + 2H]^{+}$ fragment ion is missing, whereas the $[a_6 + 2H]^{+}$ ion is abundant. CID of the charge-reduced (LRG***L***ADK + 2H)$^{+\bullet}$ again shows specific features, including loss of water, which is absent in the CID spectrum of the Pro analogue (Figure 5b). The main fragmentations on CID are loss of neutral molecules of $C_6H_{12}N_2O$ (*m/z* 645) and $C_6H_{14}N_2O_2$ (*m/z* 627). These are typical proton-driven dissociations of C-terminal Lys residues in peptide cations that indicate that the radical site in the charge-reduced ion is very stable and does not induce competitive homolytic bond cleavages.

Charge-reduced peptide ions with the *N*-terminal Arg residue (RLG***X***ADK + 2H)$^{+\bullet}$ and their dimethyl esters gave CID spectra that were to some extent analogous to those of the (LRG***X***ADK + 2H)$^{+\bullet}$ series. The Pro analog showed a loss of leucine C_3H_7 (*m/z* 714), arginine $C_3H_8N_3$ (*m/z* 671), (Lys − H)$^{\bullet}$ (*m/z* 612), and formation of the $[a_6 + 2H]^{+}$ fragment ion at *m/z* 584 (Figure 5c). These dissociations are also prominently seen in the CID spectrum of the Pro dimethyl ester with the exception of the (Lys − H)$^{\bullet}$ loss, which is absent (Supplementary Figure S24a, b). The

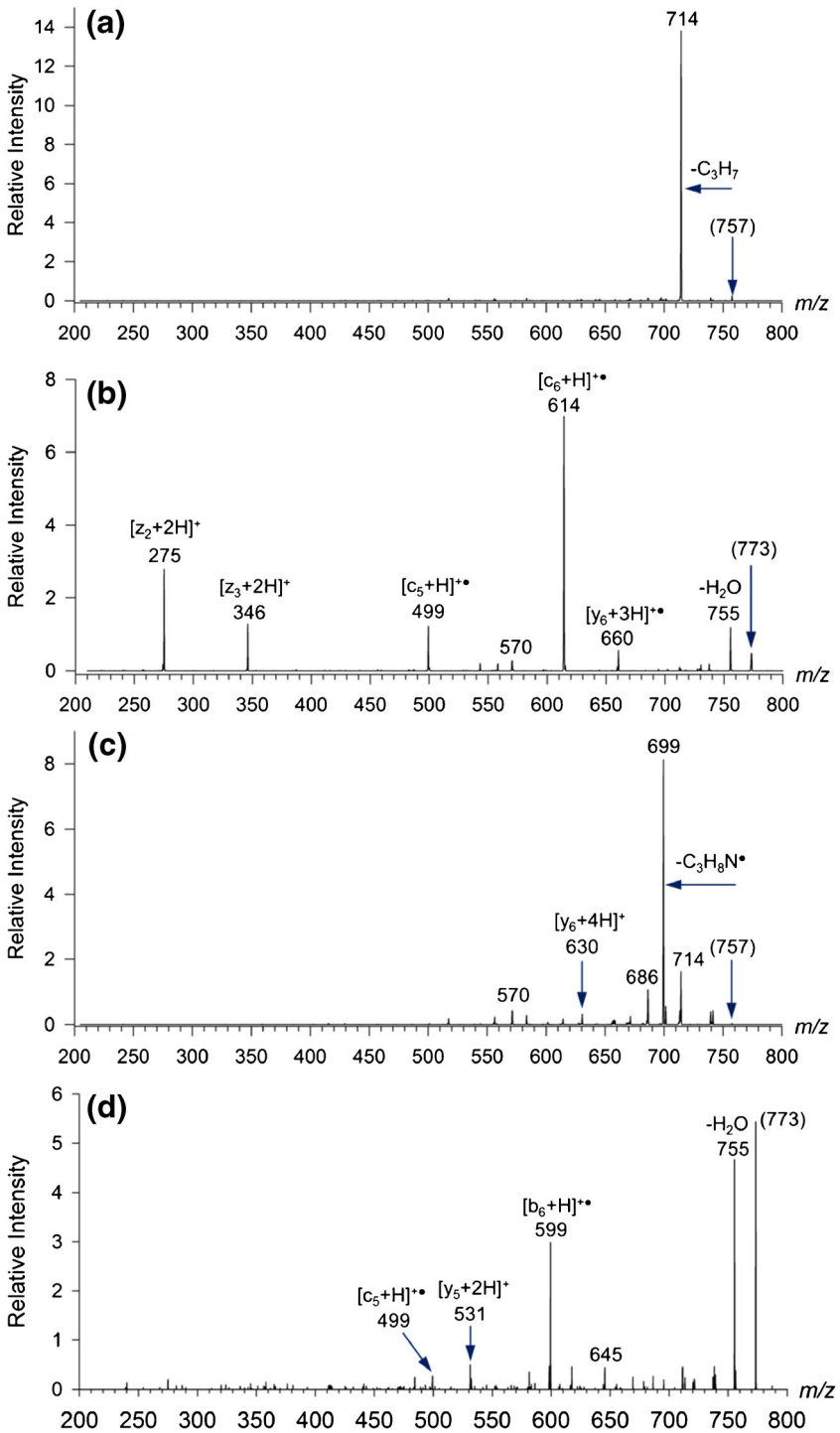

Figure 4. CID-MS^3 spectra of (**a**) (LKG***P***ADR + 2H)$^{+\bullet}$ generated by ETD of (LKG***P***ADR + 2H)$^{2+}$; (**b**) (LKG***L***ADR + 2H)$^{+\bullet}$ generated by ETD of (LKG***L***ADR + 2H)$^{2+}$; (**c**) (KLG***P***ADR + 2H)$^{+\bullet}$ generated by ETD of (KLG***P***ADR + 2H)$^{2+}$; (**d**) (KLG***L***ADR + 2H)$^{+\bullet}$ generated by ETD of (KLG***L***ADR + 2H)$^{2+}$

CID spectrum of the charge-reduced (RLGLADK + 2H)$^{+\bullet}$ shows fragment ions by loss of water and the neutral $C_6H_{12}N_2O$ (*m/z* 645) and $C_6H_{14}N_2O_2$ (*m/z* 627) molecules from the lysine residue (Figure 5d).

In summarizing this section, CID-MS^3 of charge-reduced peptide cation radicals from these heptapeptides and their dimethyl esters displayed a broad variety of different dissociations. The most salient feature was the absence of standard N–C_α backbone dissociations in all these charge-reduced peptide ions with the exception of LKG***L***ADR. Radical-induced dissociations occurred in the side chains of *N*-terminal Leu, Lys, and Arg. The Pro-4/

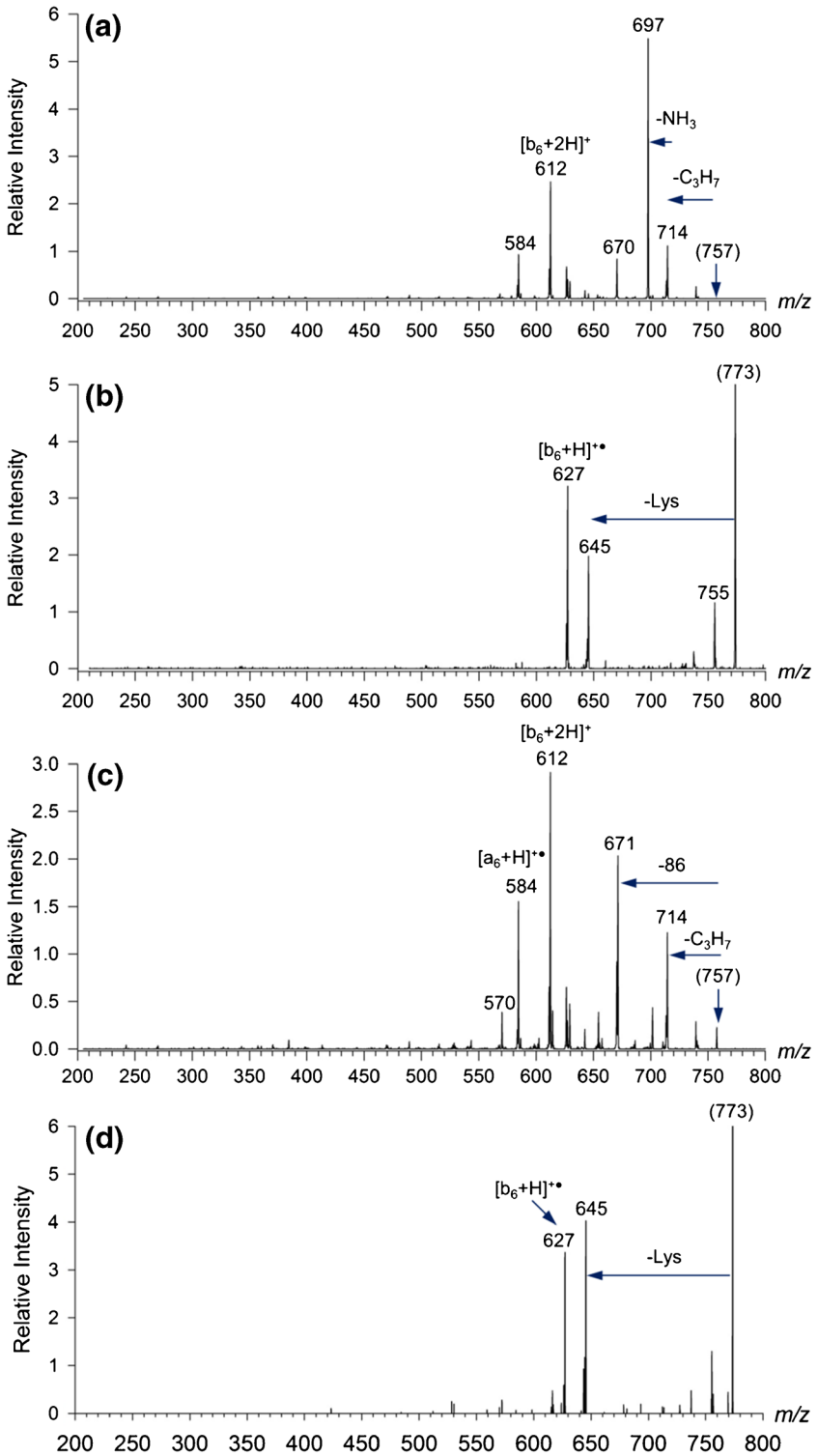

Figure 5. CID-MS^3 spectra of (**a**) (LRG***P***ADK + 2H)$^{+\bullet}$ generated by ETD of (LRG***P***ADK + 2H)$^{2+}$; (**b**) (LRG***L***ADK + 2H)$^{+\bullet}$ generated by ETD of (LRG***L***ADK + 2H)$^{2+}$; (**c**) (RLG***P***ADK + 2H)$^{+\bullet}$ generated by ETD of (RLG***P***ADK + 2H)$^{2+}$; (**d**) (RLG***L***ADK + 2H)$^{+\bullet}$ generated by ETD of (RLG***L***ADK + 2H)$^{2+}$

Leu-4 substitution had a stunningly large effect on the charge-reduced ion dissociations in that the Leu-4 containing cation-radical ions preferentially dissociated by proton driven reactions. These effects indicate that the Pro-4 and Leu-4 peptides had radical sites in different positions and with different reactivity that were created by electron attachment and (presumably) stabilizing isomerizations that formed the metastable and stable survivor cation radicals.

UVPD of Charge-Reduced Peptide Cation Radicals

Further information regarding the nature of the charge-reduced cation radicals was obtained from UVPD-MS^3 spectra at 355 nm. This excitation wavelength was chosen because it is specific for radical-based chromophores in peptides, whereas standard unmodified amino acid residues are not activated [35, 40]. UVPD at 355 nm thus provides a useful selective probe of peptide radicals. In addition, photon absorption populates excited electronic states that may dissociate on the excited state potential energy surface or undergo vibronic transition to a vibrationally excited ground electronic state of well-defined non-thermal excitation energy, $E_{exc} = E_{hv} + H_{th}$, where E_{hv} is the photon energy (3.49 eV, 337 kJ mol^{-1}) and H_{th} is the ion enthalpy at the ambient temperature in the ion trap (310 K for the LTQ).

UVPD at 355 nm of charge-reduced $(LKG\boldsymbol{P}ADR + 2H)^{+\bullet}$ showed two major dissociation channels by loss of H (74%–93%) and C_3H_7 (7-26%). The photodepletion curve of $(LKG\boldsymbol{P}ADR + 2H)^{+\bullet}$ ions that were produced by single electron transfer to $(M + 2H)^{2+}$ was bimodal (Figure 6a), composed of a fraction showing a fast exponential decay with the number of laser pulses (n), and a 31% fraction of residual, non-photoactive ions. Quantitation was carried out by a least-squares fit, $I = I_0(0.627e^{-1.92n} + 0.310)$, where I is the ion intensity relative to I_0. The photodepletion curve of $(LKG\boldsymbol{P}ADR + 2H)^{+\bullet}$ ions that were produced by double electron transfer to $(M + 3H)^{3+}$ was also bimodal (Figure 6b), showing a more gradual exponential decay with the number of laser pulses and a 24% fraction of residual, non-photoactive ions, according to the least-squares fit: $I = I_0(0.709e^{-0.434n} + 0.239)$. The bimodality and difference in the decay rates are remarkable and may indicate different compositions of isomers of the charge-reduced ions when formed by single and double electron transfer. This is despite the fact that CID of $(LKG\boldsymbol{P}ADR + 2H)^{+\bullet}$ that were generated from precursor ions of either charge state gave identical spectra that showed a dominant loss of C_3H_7, but no loss of H.

UVPD of $(KLG\boldsymbol{P}ADR + 2H)^{+\bullet}$ also showed bimodal photodepletion, forming the major fragment ions by loss of water (93%) and a 58 Da fragment (C_3H_8N, 7%) (Figure 6c, d). This branching ratio is very different from that on CID (Figure 4c), where the loss of C_3H_8N predominates and loss of water is very minor. Photodepletion of $(KLG\boldsymbol{P}ADR + 2H)^{+\bullet}$ generated from the triply charged precursor showed a faster rate and a lower residual, $I = I_0(0.879e^{-1.26n} + 0.105)$, than for the cation radical generated from the doubly charged precursor that fits $I = I_0(0.693e^{-0.4369n} + 0.256)$, as illustrated by the fit curves in Figure 6c, d. Again, this is contrary to the CID spectra of $(KLG\boldsymbol{P}ADR + 2H)^{+\bullet}$, which were identical for ions generated from precursors of either charge state.

Charge-reduced $(RLG\boldsymbol{P}ADK + 2H)^{+\bullet}$ and $(LRG\boldsymbol{P}ADK + 2H)^{+\bullet}$ underwent UVPD to dissociate by loss of H and water as the main photofragmentation channels. The molar fractions of the $(M + 2H)^{+\bullet}$ ions generated from the triply charged precursors showed an exponential decay with the number of laser pulses. The best fits for the decay curves indicated the presence of two types of components for both peptide ions, a major photoactive fraction (72%–74%) and a minor photo-inactive fraction (26%–28%) (Figure 6e, f), according to the least-square fits $I = I_0(0.739e^{-0.275n} + 0.261)$ and $I = I_0(0.724e^{-0.277n} + 0.266)$ for $(LRG\boldsymbol{P}ADK + 2H)^{+\bullet}$ and $(RLG\boldsymbol{P}ADK + 2H)^{+\bullet}$, respectively. Of note are the similar molar fractions and decay exponents for the photoactive components in both peptide ions. Also of note is that the dissociations observed on UVPD were substantially different from the CID spectra, which did not display loss of H and in which loss of water was a very minor dissociation channel (Figure 5a, c).

UV–VIS Action Spectroscopy

To further characterize the charge-reduced cation-radials, we obtained a UV–VIS photodissociation action spectrum of the most photoactive species, which was $(LKG\boldsymbol{P}ADR + 2H)^{+\bullet}$ generated from $(LKG\boldsymbol{P}ADR + 2H)^{2+}$ (Figure 7). The spectrum showed a weak absorption at 340–400 nm that chiefly resulted in the photodissociative loss of H. More abundant absorption bands, represented by both of the main dissociation channels, were found at 325, 300, 285, 265, and 250 nm. There was virtually no absorption in the visible region above 400 nm. The origin of these bands and structure assignment for the chromophores are discussed below.

CID and UVPD of Doubly Reduced Hydrogen-Super-Rich Ions

Attachment of two electrons to triply charged peptide ions of the Pro-4 series created stable $(M + 3H)^+$ ions that retained all three hydrogen atoms introduced by peptide protonation. These ions showed regular peak shapes and m/z values and could be isolated and investigated by MS^3 experiments. CID spectra showed dissociations by loss of water, ammonia, and backbone cleavages forming the $[b_6 + 2H]^+$ and $[y_4 + 4H]^+$ fragment ions from all sequences (Supplementary Figure S25a–d). These assignments were corroborated by the CID spectra of the dimethyl esters that showed +14 Da and +28 Da mass shifts for the $[b_6 + 2H]^+$ and $[y_5 + 4H]^+$ ions, respectively, consistent with the expected retention of the Asp residue in the former fragments and both the Asp and C-terminal residues in the later fragments (Supplementary Figure S26a–d). In addition, CID of $(M + 3H)^+$ ions from the Lys-terminated peptides (Supplementary Figure S25c, d) showed fragment ions formed by loss of $C_6H_{12}N_2O$, as confirmed by accurate mass measurements. All these dissociations are typical of even-electron peptide ions and point to the particularly facile proton-driven dissociations of amide bonds on the N-terminal side of the Gly residue and the C-terminal side of the Asp residue [54–56]. In contrast, no radical-induced dissociations leading to homolytic bond cleavages in the side chains or backbone were identified for the $(M + 3H)^+$ ions. Multipulse laser irradiation at 355 nm, which specifically targets peptide radical groups [35, 40], did not induce dissociation of the $(M + 3H)^+$ ions. This strongly indicates that these doubly reduced ions had closed electronic shells and were not biradicals as proposed previously for ubiquitin ions [38].

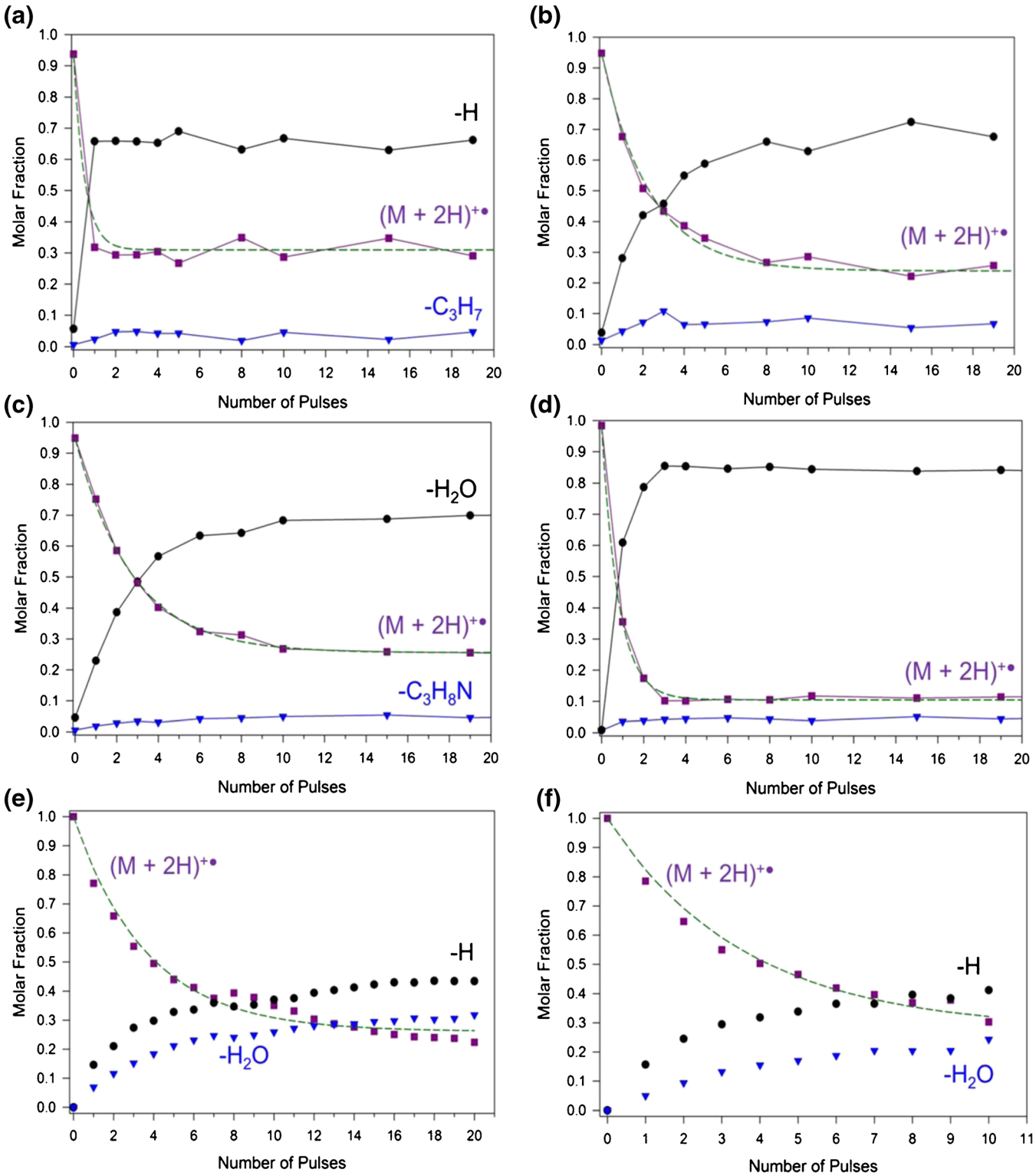

Figure 6. Photodepletion curves for $(LKG\mathbf{P}ADR + 2H)^{+\bullet}$ from (**a**) $(LKG\mathbf{P}ADR + 2H)^{2+}$ and (**b**) $(LKG\mathbf{P}ADR + 3H)^{3+}$; $(KLG\mathbf{P}ADR + 2H)^{+\bullet}$ from (**c**) $(KLG\mathbf{P}ADR + 2H)^{2+}$ and (**d**) $(LKG\mathbf{P}ADR + 3H)^{3+}$; (**e**) $(LRG\mathbf{P}ADK + 2H)^{+\bullet}$ from $(LRG\mathbf{P}ADK + 3H)^{3+}$ and (**f**) $(RLG\mathbf{P}ADK + 2H)^{+\bullet}$ from $(RLG\mathbf{P}ADK + 3H)^{3+}$. The green dash lines are least-squares exponential fits according to the formulas in the text

The backbone amide fragmentations located the two extra hydrogen atoms between the Gly and Asp residues. The absence of $(M + 3H)^+$ ions from peptides of the Leu-4 series suggested that the reductive double hydrogen addition was associated with the Pro-4 residue. The suggested ion structures and mechanisms are discussed later in the paper.

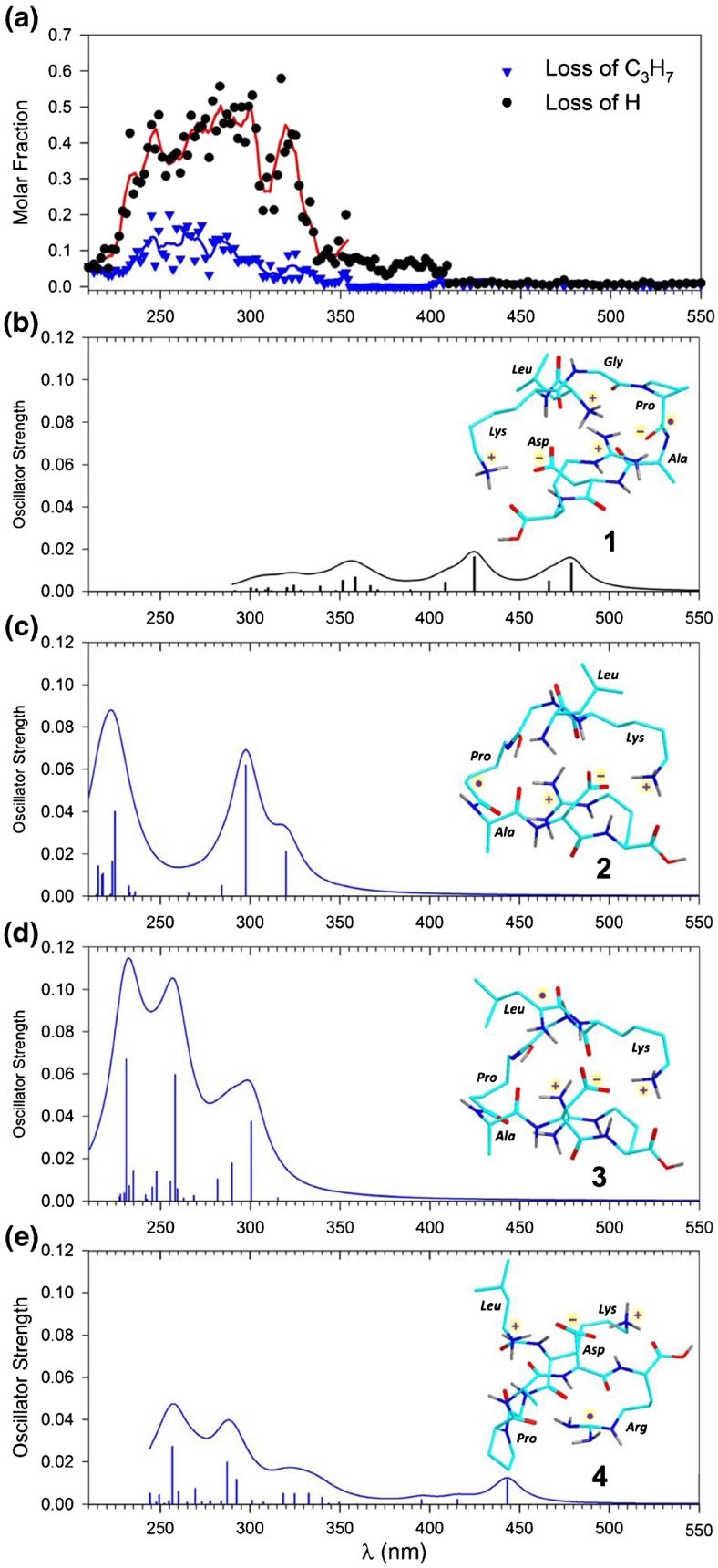

Figure 7. (**a**) UV–VIS action spectrum of $(LKG\boldsymbol{P}ADR + 2H)^{+\bullet}$ generated by electron transfer to $(LKG\boldsymbol{P}ADR + 2H)^{2+}$; (**b**)–(**e**) TD-DFT/B97X-D/6-311++G(2d,p) calculated absorption spectra of cation-radical isomers **1**, **2**, **3**, and **4**

Ion Molecule Reactions with O_2

Ion-molecule reactions with residual dioxygen have been previously suggested as a detector for radical sites in charge-reduced peptide [37], protein [38], and fragment ions of the z type [67]. When applied to the $(M + 2H)^{+\bullet}$ and $(M + 3H)^{+}$ ions from the peptides under study, we isolated the ions of interest in the ion trap and allowed them to react with the residual gas for 2 s without excitation. These experiments produced virtually no (<0.1%) dioxygen adducts. As control experiments, we also isolated several $[z_n + H]^{+\bullet}$ ions from ETD and allowed them to react with the residual gas in the ion trap for 2 s. Reactions of the $[z_n + H]^{+\bullet}$ ions produced 2%–5% of dioxygen adducts, indicating that the oxygen partial pressure in the ion trap was sufficient for reactive radicals. The negative results for the $(M + 2H)^{+\bullet}$ ions indicated that our charge-reduced peptide ions had radical-carrying groups that were nonreactive towards dioxygen. These results are consistent with previous reports by Julian and co-workers [68], and O'Hair et al. [69], that reactions with O_2 are not an unequivocal test for peptide cation radicals. Other radical-reactive gases may be more reliable to characterize hydrogen-rich peptide cation radicals [69, 70]. The results for the $(M + 3H)^{+}$ ions were consistent with their CID and UVPD that both pointed to the closed shell nature of these ions and excluded biradical structures.

Discussion

The above-described experiments disclosed several major effects regarding the structure and reactivity of the charge-reduced peptide cation radicals. The first major feature is the different properties of the Pro- and Leu-containing radicals. This is reflected by the fractions of metastable ions as well as the mass shifts, both pointing to the much lower stability of the charge-reduced ions lacking the Pro residue. These effects raise the question of where the electron goes upon transfer in the ion–ion reaction, which we specifically address with the (LKG-***P***ADR + 2H)$^{2+}$ ions.

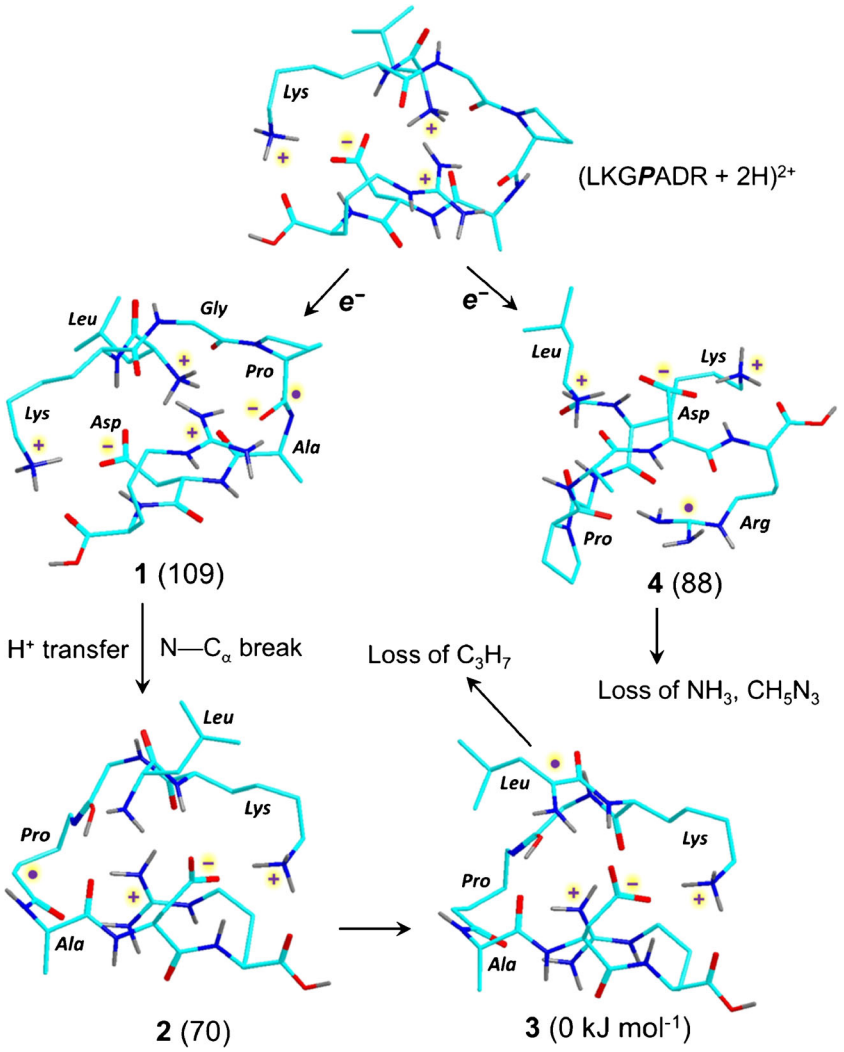

Scheme 2. Structures, reactions, and relative energies of charge-reduced $(LKGPADR + 2H)^{+\bullet}$ ions

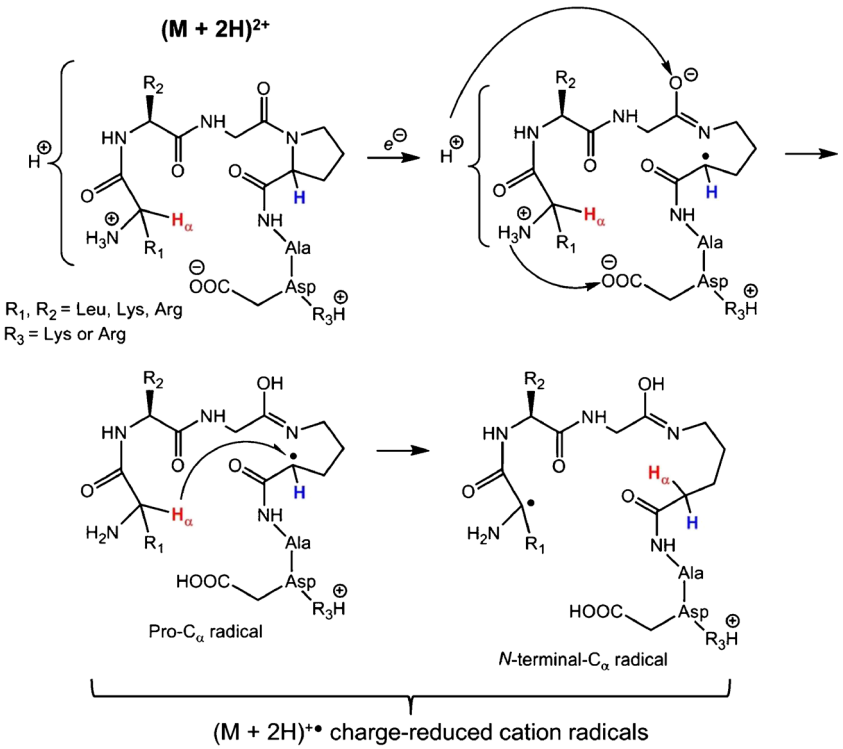

Scheme 3. Generic scheme of electron transfer, proline ring opening, and stabilizing proton and hydrogen migrations in Pro-containing singly charge-reduced peptide ions from $(M + 2H)^{2+}$

Where Does the Electron Go?

We use the analysis of the ETD spectrum to assign dissociations that are triggered by electron attachment to particular functional groups in the ion. Loss of ammonia occurs upon electron attachment to the *N*-terminal ammonium and Arg guanidinium groups [40, 53, 71], accounting for 23% of fragment ion intensity in the ETD spectrum of (LKG***P***ADR + 2H)$^{2+}$. Both these charged groups are present in the (LKG-***P***ADR + 2H)$^{2+}$ ions, which prefer zwitterionic structures such as the one shown in Scheme 2 [39]. Electron attachment to the Arg guanidinium group can form radical **4**, which is a relatively high-energy structure that can photodissociate by loss of H

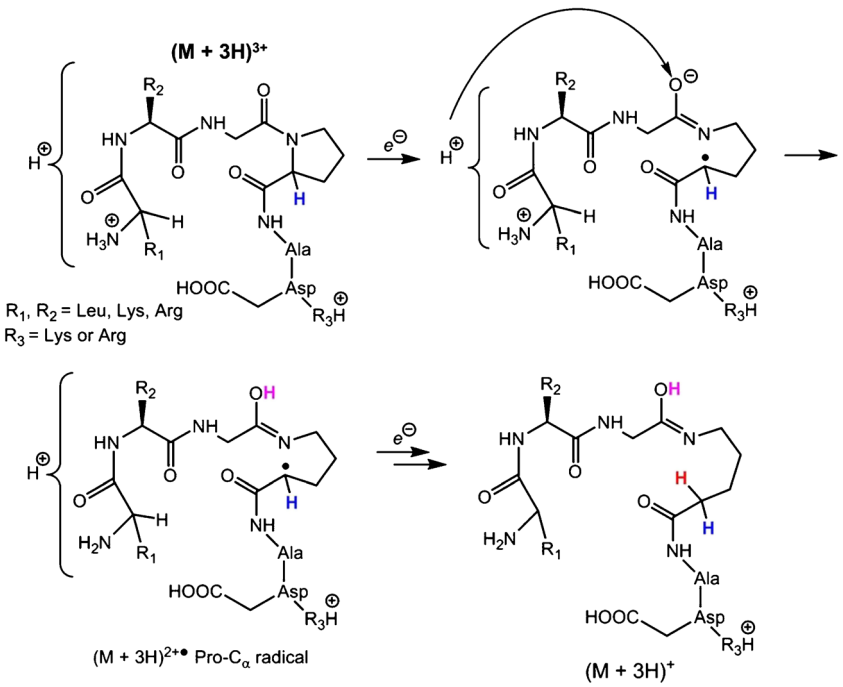

Scheme 4. Generic scheme of electron transfer, proline ring opening, stabilizing proton, and hydrogen migrations in Pro-containing doubly charge-reduced peptide ions from $(M + 3H)^{3+}$

from an excited electronic state [72]. The TD-DFT-calculated UV–VIS spectrum of **4** (Figure 7e) showed absorption bands at 300–350 nm, which can lead to light absorption and UVPD by the 355 nm laser line. The energetics of ground-state Arg radicals, such as **4**, favors loss of guanidine (CH_5N_3) upon CID, as this is the lowest transition state energy dissociation (E_{TS} = 73 kJ mol^{-1}) [72]. However, loss of guanidine is represented by only 4% in the ETD spectrum of (LKG***P***ADR + 2H)$^{2+}$ and is absent in the CID spectrum of (LKG***P***ADR + 2H)$^{+\bullet}$ (Figure 4a). This indicates that electron attachment to the Arg charged group is a minor process, but does not exclude that structure **4** is represented in a fraction of the charge-reduced cation radicals. Electron transfer to the backbone amide groups is thought to result in backbone N–C_α bond cleavage according to the Utah-Washington model [73, 74]. The backbone fragments account for 25% in the ETD spectrum of (LKG***P***ADR + 2H)$^{2+}$. However, a prominent feature of the 48% fraction of surviving heptapeptide cation radicals is the lack of backbone dissociations upon further activation. This clearly suggests that electron transfer does not produce noncovalent ion–molecule [z + c] complexes from these heptapeptide ions with the singular exception of LKG***L***ADR. Thus, despite their fragility, the charge-reduced species are most likely covalent radicals.

The collision- and light-induced dissociations of the charge-reduced peptide cation radicals are sequence-specific, pointing to different structures for the radical intermediates that developed as a result of electron attachment. We will discuss the individual peptide sequences from the point of view of the observed dissociations induced by vibrational excitation under slow heating conditions and electronic excitation upon photon absorption. Our basic premise is that electron attachment occurs in the Pro amide group forming a high-energy zwitterionic intermediate of type **1** (referring to Scheme 2), which undergoes exothermic proton transfer and N–C_α bond cleavage in the Pro ring to form the Pro radical of the type **2**. Further rearrangements by hydrogen atom migrations can lead to lower-energy intermediates such as the Leu C_α radical **3** or its *N*-terminal Lys and Arg analogues from the other peptide sequences. These isomerizations are generically sketched in Scheme 3 that tracks the presumed proton and hydrogen atom migrations. We cannot resolve which charged groups are involved in these proton migrations, although the final structures of the Pro- and *N*-terminal C_α radicals are presumed to be protonated at the basic Arg residue, as shown in Scheme 3.

Regarding the stable doubly reduced ions, (M + 3H)$^{+}$, they showed all features of even-electron ions lacking radical functionalities. This is corroborated by the absence of radical chromophores in these ions, their inert behavior toward O_2, and CID spectra that showed typical proton-driven fragmentations. The formation of even-electron species upon double-electron transfer to (M + 3H)$^{3+}$ ions is sketched in Scheme 4. This presumes initial electron attachment in the Pro amide group followed by ring cleavage and proton migrations, forming doubly charged analogues of Pro C_α radical ions (Scheme 4). Upon further electron attachment to one of the remaining charged groups, the Pro C_α radical can function as a hydrogen atom acceptor, forming a Pro C_α-CH_2 group in a closed-shell (M + 3H)$^{+}$ product. Mechanistic details of these isomerizations are not specified in the generic Scheme 4, and their elucidation would require a substantial effort, which is beyond the scope of this work.

Case in Point: UV–VIS Action Spectrum and Structure of (LKGPADR + 2H)$^{+\bullet}$

CID and UVPD of (LKGPADR + 2H)$^{+\bullet}$ triggered different major dissociations, which were, respectively, the loss of C_3H_7 and H radicals. The photodepletion curve at the selective 355 nm wavelength clearly pointed to two or more isomeric cation radicals being present in the ion population. This complicated the assignment of the UV–VIS action spectrum (Figure 7a). We used time-dependent DFT calculations to obtain UV–VIS absorption spectra of several candidate structures. Because of the prominent proline effect, we focused on radicals developed by an initial electron attachment to the Pro amide group in (LKGPADR + 2H)$^{2+}$ (Scheme 2). The precursor ion prefers zwitterionic structures with positive charges on the basic *N*-terminal, Lys, and Arg groups and a negative charge at the Asp carboxylate [39]. Electron attachment to the Pro amide can produce a double zwitterion (**1**, Figure 7b); however, the calculated absorption spectrum of **1** (Figure 7b) showed multiple bands in the visible region with maxima at 425 and 478 nm that were not represented in the action spectrum of the charge-reduced ion (Figure 7a). Proton transfer from the *N*-terminus, followed by Pro ring opening by N–C_α bond cleavage [75] was 38 kJ mol^{-1} exothermic, forming cation-radical **2** (Scheme 2). The absorption bands at 295 and 320 nm in the calculated UV–VIS spectrum of **2** (Figure 7c) are associated with excitations within the Pro C_α-CO-NH- radical and have counterparts in the same wavelength region of the action spectrum. However, the 230–280 nm region in the calculated spectrum of **2** showed no strong absorption bands that would match the action spectrum. A further isomerization of **2** by Leu-C_α-H transfer (Scheme 2) was 70 kJ mol^{-1} exothermic yielding isomer **3**, which was a Leu-C_α radical. The calculated absorption spectrum of **3** (Figure 7d) showed major bands at 230, 258, and 301 nm, which were represented in the action spectrum of (LKGPADR + 2H)$^{+\bullet}$. Hence, the low-energy isomer **3** accounts for some of the major features in the action spectrum. The bimodal photodepletion curve at 355 nm can be explained by the presence of **2** and **3** in the ion population. Radical **2** shows an absorption band at 325 nm that is likely to be extended to 355 nm by vibronic broadening to account for photodissociation at this wavelength. In contrast, radical **3** has only a very weak absorption band at 316 nm that cannot account for photodissociation at 355 nm. Hence, the UVPD data point to a mixture of **2** and **3** being produced by electron attachment, Pro ring opening, and partial isomerization by H-atom migration. The molar fractions of **2** and **3** are not directly deducible from the photodepletion curves

(Figure 6a, b) because of the possibility of exothermic isomerization of **2** to **3** that would result in photobleaching. The different dissociation channels on CID and UVPD are consistent with the nature of these excitations and the dissociation energetics. Loss of H is a relatively high-energy dissociation (E_{TS} > 210 kJ mol^{-1}) [45] that is driven by photon absorption but is absent on CID. In contrast, CID is expected to trigger direct loss of C_3H_7 from Leu side chain in the Leu-C_α radical **3** [64–66], or drive the exothermic isomerization of **2** to **3** followed by loss of C_3H_7 from the latter.

The observed UVPD at 355 nm of the other sequence variants (Figure 6c–f) implied that the charge-reduced ions contained radical-associated chromophores formed by electron attachment. Analysis by TD-DFT calculations of $(KLGPADR + 2H)^{+\bullet}$ ions **5**–**9** indicated absorption bands at λ > 300 nm in the Pro and Lys radicals **5**, **6**, and **7**, **8**, respectively, that can account for the observed photodissociation (Supplementary Figure S27a–c). In contrast, the photodissociation fragment ion by loss of water **9** is calculated not to absorb light at 355 nm, which is consistent with its permanence in the pulse-dependent experiments (Figure 6c, d).

Comparison of CID and UVPD

UVPD at 355 nm of $(KLGPADR + 2H)^{+\bullet}$ induced the loss of water and C_3H_8N radical from the Lys side chain (Figure 6c, d). Loss of water can be proton-driven; however, it does not occur competitively upon CID (Figure 4c), which suggests a radical mechanism. To establish the origin of the water molecule, one would have to undertake an ^{18}O labeling study, which we have not done. However, the photochemical properties of this fragment are consistent with structure **9** representing an α,β-conjugated acyl radical formed in the Arg residue (Supplementary Figure S28). In contrast, CID is dominated by loss of the Lys C_3H_8N radical, indicating a Lys C_α radical intermediate, such as **7** or **8** formed by isomerization of a primary charge-reduced cation radical.

UVPD at 355 nm of $(LRGPADK + 2H)^{+\bullet}$ and $(RLGPADK + 2H)^{+\bullet}$ gave similar results in that it promoted loss of H and water as the major photodissociations (Figure 6e, f). The CID spectra were very different in that they showed a combination of radical dissociations in the side chains, loss of C_3H_7 and C_3H_8N radicals from Leu and Lys, respectively, and proton driven backbone cleavage at the Asp residue giving the prominent $[b_6 + 2H]^+$ ion by loss of a $(Lys - H)^\bullet$ radical (Figure 5a, c). These differences indicate that UVPD occurred in stable charge-reduced cation radicals, whereas CID induced radical isomerizations leading to intermediates for the observed dissociations.

Conclusions

This combined experimental and computational study allows us to arrive at the following conclusions. The Pro and Leu residues in the peptides under study have a critical effect on the stability of $(M + 2H)^{+\bullet}$ and $(M + 3H)^+$ ions produced by non-dissociative electron transfer to doubly and triply protonated ions. Charge-reduced $(M + 2H)^{+\bullet}$ and $(M + 3H)^+$ ions having the Pro residue are stable, and this stabilization by the Pro-4 residue is attributed to the electron-induced opening of the Pro ring followed by radical rearrangements by hydrogen atom and proton migrations. Charge-reduced $(M + 2H)^{+\bullet}$ ions having the Leu-4 residue were predominantly metastable while no $(M + 3H)^+$ ions were detected. Photodissociation at 355 nm of $(M + 2H)^{+\bullet}$ ions revealed major populations of photoactive species with minor admixtures of photostable isomers. UV–VIS photodissociation action spectroscopy was used to characterize photoactive $(LKGPADR + 2H)^{+\bullet}$ cation radicals as a mixture of C_α-radical species of different UV absorption spectra.

Acknowledgments

Support by the Chemistry Division of the National Science Foundation (Grant CHE-1359810 to F.T.) is gratefully acknowledged. F.T. thanks the Klaus and Mary Ann Saegebarth Endowment for additional support.

References

1. Voicescu, M., El Khoury, Y., Martel, D., Heinrich, M., Hellwig, P.: Spectroscopic analysis of tyrosine derivatives: on the role of the tyrosine-histidine covalent linkage in cytochrome c oxidase. J. Phys. Chem. B **113**, 13429–13436 (2009)
2. Sjoberg, B.M., Reichard, P., Graslund, A., Ehrenberg, A.: Nature of the free radical in ribonucleotide reductase from *Escherichia coli*. J. Biol. Chem. **252**, 536–541 (1977)
3. Knappe, J., Sawers, G.: A radical-chemical route to acetyl-CoA: the anaerobically induced pyruvate formate-lyase system of *Escherichia coli*. FEMS Microbiol. Rev. **6**, 383–398 (1990)
4. Sawers, G., Watson, G.: A glycyl radical solution: oxygen-dependent interconversion of pyruvate formate-lyase. Mol. Microbiol. **29**, 945–954 (1998)
5. Whittaker, M.M., DeVito, V.L., Asher, S.A., Whittaker, J.W.: Resonance Raman evidence for tyrosine involvement in the radical site of galactose oxidase. J. Biol. Chem. **264**, 7104–7106 (1989)
6. Ulas, G., Lemmin, T., Wu, Y., Gassner, G.T., DeGrado, W.F.: Designed metalloprotein stabilizes a semiquinone radical. Nature Chem. **8**, 354–359 (2016)
7. Moore, G.F., Hambourger, M., Gervaldo, M., Poluektov, O.G., Rajh, T., Gust, D., Moore, T.A., Moore, A.L.: A bioinspired construct that mimics the proton coupled electron transfer between P680•+ and the TyrZ-His190 pair of photosystem II. J. Am. Chem. Soc. **130**, 10466–10467 (2008)
8. Stubbe, J., van der Donk, W.A.: Protein radicals in enzyme catalysis. Chem. Rev. **98**, 705–762 (1998)
9. Dorcak, V., Palecek, E.: Chronopotentiometric determination of redox states of peptides. Electroanalysis **19**, 2405–2412 (2007)
10. Horsley, J.R., Yu, J., Moore, K.E., Shapter, J.G., Abell, A.D.: Unraveling the interplay of backbone rigidity and electron rich side-chains on electron transfer in peptides: the realization of tunable molecular wires. J. Am. Chem. Soc. **136**, 12479–12488 (2014)
11. Barr, I., Latham, J.A., Iavarone, A.T., Chantarojsiri, T., Hwang, J.D., Klinman, J.P.: Demonstration that the radical S-adenosylmethionine (SAM) enzyme PqqE catalyzes de novo carbon-carbon cross-linking within a peptide substrate PqqA in the presence of the peptide chaperone PqqD. J. Biol. Chem. **291**, 8877–8884 (2016)
12. Green, M.C., Dubnicka, L.J., Davis, A.C., Rypkema, H.A., Francisco, J.S., Slipchenko, L.V.: Thermodynamics and kinetics for the free radical oxygen protein oxidation pathway in a model for β-structured peptides. J. Phys. Chem. A **120**, 2493–2503 (2016)
13. Bruender, N.A., Wilcoxen, J., Britt, R.D., Bandarian, V.: Biochemical and spectroscopic characterization of a radical S-adenosyl-L-methionine

enzyme involved in the formation of a peptide thioether cross-link. Biochemistry **55**, 2122–2134 (2016)
14. Kruger, N.A., Zubarev, R.A., Horn, D.M., McLafferty, F.W.: Electron capture dissociation of multiply charged peptide cations. Int. J. Mass Spectrom. **185/186/187**, 787–793 (1999)
15. Tureček, F.: N–C_α bond dissociation energies and kinetics in amide and peptide radicals. Is the dissociation a nonergodic process? J. Am. Chem. Soc. **125**, 5954–5963 (2003)
16. Coon, J.J., Ueberheide, B., Syka, J.E.P., Dryhurst, D.D., Ausio, J., Shabanowitz, J., Hunt, D.F.: Protein identification using sequential ion/ion reactions and tandem mass spectrometry. Proc. Natl. Acad. Sci. U. S. A. **102**, 9463–9468 (2005)
17. Hakansson, K., Chalmers, M.J., Quinn, J.P., McFarland, M.A., Hendrickson, C.L., Marshall, A.G.: Combined electron capture and infrared multiphoton dissociation for multistage MS/MS in a Fourier transform ion cyclotron resonance mass spectrometer. Anal. Chem. **75**, 3256–3262 (2003)
18. Syka, J.E.P., Coon, J.J., Schroeder, M.J., Shabanowitz, J., Hunt, D.F.: Peptide and protein sequence analysis by electron transfer dissociation mass spectrometry. Proc. Natl. Acad. Sci. U. S. A. **101**, 9528–9533 (2004)
19. Zubarev, R.A., Kelleher, N.L., McLafferty, F.W.: Electron capture dissociation of multiply charged protein cations. A nonergodic process. J. Am. Chem. Soc. **120**, 3265–3266 (1998)
20. Oh, H.-B., Breuker, K., Sze, S.K., Ge, Y., Carpenter, B.K., McLafferty, F.W.: Secondary and tertiary structures of gaseous protein ions characterized by electron capture dissociation mass spectrometry and photofragment spectroscopy. Proc. Natl. Acad. Sci. U. S. A. **99**, 15863–15868 (2002)
21. Gunawardena, H.P., He, M., Chrisman, P.A., Pitteri, S.J., Hogan, J.M., Hodges, B.D.M., McLuckey, S.A.: Electron transfer versus proton transfer in gas-phase ion/ion reactions of polyprotonated peptides. J. Am. Chem. Soc. **127**, 12627–12639 (2005)
22. Liu, J., Gunawardena, H.P., Huang, T.-Y., McLuckey, S.A.: Charge-dependent dissociation of insulin cations via ion/ion electron transfer. Int. J. Mass Spectrom. **276**, 160–170 (2008)
23. Xia, Y., Gunawardena, H.P., Erickson, D.E., McLuckey, S.A.: Effects of cation charge-site identity and position on electron-transfer dissociation of polypeptide cations. J. Am. Chem. Soc. **129**, 12232–12243 (2007)
24. Tureček, F., Jones, J.W., Towle, T., Panja, S., Nielsen, S.B., Hvelplund, P., Paizs, B.: Hidden histidine rearrangements upon electron transfer to gas-phase peptide ions. Experimental evidence and theoretical analysis. J. Am. Chem. Soc. **130**, 14584–14596 (2008)
25. Chung, T.W., Tureček, F.: Amplified histidine effect in electron-transfer dissociation of histidine-rich peptides from histatin 5. Int. J. Mass Spectrom. **306**, 99–107 (2011)
26. Tureček, F., Panja, S., Wyer, J.A., Ehlerding, A., Zettergen, H., Nielsen, S.B., Hvelplund, P., Bythell, B., Paizs, B.: Carboxyl-catalyzed prototropic rearrangements in histidine peptide radicals upon electron transfer. Effects of peptide sequence and conformation. J. Am. Chem. Soc. **131**, 16472–16487 (2009)
27. Marek, A., Pepin, R., Peng, B., Laszlo, K.J., Bush, M.F., Tureček, F.: Electron transfer dissociation of photolabeled peptides. Backbone cleavages compete with diazirine ring rearrangements. J. Am. Soc. Mass Spectrom. **24**, 1641–1653 (2013)
28. Viglino, E., Lai, C.K., Mu, X., Chu, I.K.; Tureček, F.: Ground and excited-electronic-state dissociations of hydrogen-rich and hydrogen-deficient tyrosine peptide cation radicals. J. Am. Soc. Mass Spectrom. **27**, 1454–1467 (2016)
29. Swaney, D.L., McAlister, G.C., Wirtala, M., Schwartz, J.C., Syka, J.E.P., Coon, J.J.: Supplemental activation method for highly efficient electron transfer dissociation of doubly protonated peptide precursors. Anal. Chem. **79**, 477–485 (2007)
30. Xia, Y., Han, H., McLuckey, S.A.: Activation of intact electron-transfer products of polypeptides and proteins in cation transmission mode ion/ion reactions. Anal. Chem. **80**, 1111–1117 (2008)
31. Brodbelt, J.S.: Photodissociation mass spectrometry: new tools for characterization of biological molecules. Chem. Soc. Rev. **43**, 2757–2783 (2014)
32. Ledvina, A.R., McAlister, G.C., Gardner, M.W., Smith, S.I., Madsen, J.A., Schwartz, J.C., Stafford Jr., G.C., Syka, J.E.P., Brodbelt, J.S., Coon, J.J.: Infrared photoactivation reduces peptide folding and hydrogen-atom migration following ETD tandem mass spectrometry. Angew. Chem. Int. Ed. **48**, 8526–8528 (2009)
33. Ledvina, A.R., Beauchene, N.A., McAlister, G.C., Syka, J.E.P., Schwartz, J.C., Griep-Raming, J., Westphall, M.S., Coon, J.J.: Activated ion electron transfer dissociation improves the ability of electron transfer dissociation to identify peptides in a complex mixture. Anal. Chem. **82**, 10068–10074 (2010)
34. Chu, I.K., Siu, C.-K., Lau, J.K.-C., Tang, W.K., Mu, X., Lai, C.K., Guo, X., Wang, X., Li, N., Yao, Z., Xia, Y., Kong, X., Oh, H.-B., Ryzhov, V., Tureček, F., Hopkinson, A.C., Siu, K.W.M.: Proposed nomenclature for peptide ion fragmentation. Int. J. Mass Spectrom. **390**, 24–27 (2015)
35. Nguyen, H.T.H., Shaffer, C.J., Tureček, F.: Probing peptide cation radicals by near-UV photodissociation in the gas phase. Structure elucidation of histidine radical chromophores formed by electron transfer reduction. J. Phys. Chem. B **119**, 3948–3961 (2015)
36. Kleinnijenhuis, A.J., Heck, A.J.R., Duursma, M.C., Heeren, R.M.A.: Does double electron capture lead to the formation of biradicals? An ECD-SORI-CID study on lacticin 481. J. Am. Soc. Mass Spectrom. **16**, 1595–160 (2005)
37. Xia, Y., Chrisman, P.A., Pitteri, S.J., Erickson, D.E., McLuckey, S.A.: Ion/molecule reactions of cation radicals formed from protonated polypeptides via gas-phase ion/ion electron transfer. J. Am. Chem. Soc. **128**, 11792–11798 (2006)
38. Baba, T., Campbell, J.L.: Capturing polyradical protein cations after an electron capture event: evidence for their stable distonic structures in the gas phase. J. Am. Soc. Mass Spectrom. **26**, 1695–1701 (2015)
39. Pepin, R., Laszlo, K.J., Marek, A., Peng, B., Bush, M.F., Lavanant, H., Afonso, C., Turecek, F.: Toward a rational design of highly folded peptide cation conformations. 3D gas-phase ion structures and ion mobility characterization. J. Am. Soc. Mass Spectrom. **27**, 1647–1660 (2016)
40. Shaffer, C.J., Marek, A., Pepin, R., Slováková, K., Tureček, F.: Combining UV photodissociation with electron transfer for peptide structure analysis. J. Mass Spectrom. **50**, 470–475 (2015)
41. Shaffer, C.J., Pepin, R., Tureček, F.: Combining UV photodissociation action spectroscopy with electron transfer dissociation for structure analysis of gas-phase peptide cation radicals. J. Mass Spectrom. **50**, 1438–1442 (2015)
42. Antoine, R., Dugourd, P.: Visible and ultraviolet spectroscopy of gas phase protein ions. Phys. Chem. Chem. Phys. **13**, 16494–16509 (2011)
43. Antoine, R., Dugourd, P.: UV-visible activation of biomolecular ions. (Laser Photodissociation and Spectroscopy of Mass-Separated Biomolecular Ions) Lect. Notes Chem. **83**, 93–116 (2013)
44. Nguyen, H.T.H., Shaffer, C.J., Pepin, R., Tureček, F.: UV action spectroscopy of gas-phase peptide radicals. J. Phys. Chem. Lett. **6**, 4722–4727 (2016)
45. Viglino, E., Shaffer, C.J., Tureček, F.: UV–VIS action spectroscopy and structures of tyrosine peptide cation radicals in the gas phase. Angew. Chem. Int. Ed. **55**, 7469–7473 (2016)
46. Hartmer, R., Kaplan, D.A., Gebhardt, C.R., Ledertheil, T., Brekenfeld, A.: Multiple ion/ion reactions in the 3D ion trap: selective reagent anion production for ETD and PTR from a single compound. Int. J. Mass Spectrom. **276**, 82–90 (2008)
47. Chai, J.D., Head-Gordon, M.: Long-range corrected hybrid density functionals with damped atom-atom dispersion corrections. Phys. Chem. Chem. Phys. **10**, 6615–6620 (2008)
48. Furche, F., Ahlrichs, A.: Adiabatic time-dependent density functional methods for excited state properties. J. Chem. Phys. **117**, 7433–7447 (2002)
49. Turecek, F.: Benchmarking electronic excitation energies and transitions in peptide radicals. J. Phys. Chem. A **119**, 10101–10111 (2015)
50. Frisch, M.J., Trucks, G.W., Schlegel, H.B.;, Scuseria, G.E., Robb, M.A., Cheeseman, J.R., Scalmani, G., Barone, V., Mennucci, B., Petersson, G.A., Nakatsuji, H., Caricato, M., Li, X., Hratchian, H.P., Izmaylov, A.F., Bloino, J., Zheng, G., Sonnenberg, J.L., Hada, M., Ehara, M., Toyota, K., Fukuda, R., Hasegawa, J., Ishida, M., Nakajima, T., Honda, Y., Kitao, O., Nakai, H., Vreven, T., Montgomery, J.A., Jr., Peralta, J.E., Ogliaro, F., Bearpark, M., Heyd, J.J., Brothers, E., Kudin, K.N., Staroverov, V.N., Kobayashi, R., Normand, J., Raghavachari, K., Rendell, A., Burant, J. C., Iyengar, S.S., Tomasi, J., Cossi, M., Rega, N., Millam, J.M., Klene, M., Knox, J.E., Cross, J.B., Bakken, V., Adamo, C., Jaramillo, J., Gomperts, R., Stratmann, R.E., Yazyev, O., Austin, A.J., Cammi, R., Pomelli, C., Ochterski, J.W., Martin, R.L., Morokuma, K., Zakrzewski, V. G., Voth, G.A., Salvador, P., Dannenberg, J.J., Dapprich, S., Daniels, A.D., Farkas, O., Foresman, J. B., Ortiz, J. V., Cioslowski, J., Fox, D.J.: Gaussian 09, Revision A.02. Gaussian Inc.: Wallingford CT (2009)
51. Roepstorff, P., Fohlman, J.: Proposal for a common nomenclature for sequence ions in mass spectra of peptides. Biomed. Mass Spectrom. **11**, 601 (1984)

52. Biemann, K.: Nomenclature for peptide fragment ions (positive ions). Methds. Enzymol. **193**, 886–887 (1990)
53. Tureček, F., Julian, R.R.: Peptide radicals and cation radicals in the gas phase. Chem. Rev. **113**, 6691–6733 (2013)
54. Yu, W., Vath, J.E., Huberty, M.C., Martin, S.A.: Identification of the facile gas-phase cleavage of the Asp-Pro and Asp-Xxx peptide bonds in matrix-assisted laser desorption time-of-flight mass spectrometry. Anal. Chem. **65**, 3015–3023 (1993)
55. Lee, S.-W., Kim, H.S., Beauchamp, J.L.: Salt bridge chemistry applied to gas-phase peptide sequencing: selective fragmentation of sodiated gas-phase peptide ions adjacent to aspartic acid residues. J. Am. Chem. Soc. **120**, 3188–3195 (1998)
56. Qin, J., Chait, B.T.: Preferential fragmentation of protonated gas-phase peptide ions adjacent to acidic amino acid residues. J. Am. Chem. Soc. **117**, 5411–5412 (1995)
57. Pepin, R., Laszlo, K.J., Peng, B., Marek, A., Bush, M.F., Tureček, F.: Comprehensive analysis of Gly-Leu-Gly-Gly-Lys peptide dication structures and cation-radical dissociations following electron transfer: from electron attachment to backbone cleavage, ion molecule complexes and fragment separation. J. Phys. Chem. A **118**, 308–324 (2014)
58. Tsybin, Y.O., Haselmann, K.F., Emmett, M.R., Hendrickson, C.L., Marshall, A.G.: Charge location directs electron capture dissociation of peptide dications. J. Am. Soc. Mass Spectrom. **17**, 1704–1711 (2006)
59. McClellan, J.E., Murphy III, J.P., Mulholland, J.J., Yost, R.A.: Effects of fragile ions on mass resolution and on isolation for tandem mass spectrometry in the quadrupole ion trap mass spectrometer. Anal. Chem. **74**, 402–412 (2002)
60. Schwartz, J.C., Senko, M.W., Syka, J.E.P.: A Two dimensional quadrupole ion trap mass spectrometer. J. Am. Soc. Mass Spectrom. **13**, 659–669 (2002)
61. Kaiser Jr., R.E., Louris, J.N., Amy, J.W., Cooks, R.G.: Extending the mass range of the quadrupole ion trap using axial modulation. Rapid Commun. Mass Spectrom. **3**, 225–229 (1989)
62. Chung, T.W., Hui, R., Ledvina, A.R., Coon, J.J., Tureček, F.: Cascade dissociations of peptide cation radicals. Part 1. Scope and effects of amino acid residues in penta-, nona-, and decapeptides. J. Am. Soc. Mass Spectrom. **23**, 1336–1350 (2012)
63. Pham, H.T., Julian, R.R.: Mass shifting and radical delivery with crown ether attachment for separation and analysis of phosphatidylethanolamine lipids. Anal. Chem. **86**, 3020–3027 (2014)
64. Vaisar, T., Gatlin, C.L., Rao, R.D., Seymour, J.L., Tureček, F.: Sequence information, distinction and quantitation of C-terminal leucine and isoleucine in ternary complexes of tripeptides with Cu(II) and 2,2'-bipyridine. J. Mass Spectrom. **36**, 306–316 (2001)
65. Fung, Y.M.E., Chan, T.-W.D.: Experimental and theoretical investigations of the loss of amino acid side chains in electron capture dissociation. J. Am. Soc. Mass Spectrom. **16**, 1523–1535 (2005)
66. Pepin, R., Tureček, F.: Kinetic ion thermometers for electron transfer dissociation. J. Phys. Chem. B **119**, 2818–2826 (2015)
67. Liu, J., Liang, X., McLuckey, S.A.: On the value of knowing a $z^{\bullet}$ ion for what it is. J. Proteome Res. **7**, 130–137 (2008)
68. Moore, B.N., Blanskby, S.J., Julian, R.R.: Ion-molecule reactions reveal facile radical migration in peptides. Chem. Commun. 5015–5017, (2009)
69. Barlow, C.K., Wright, A., Easton, C.J., O'Hair, R.A.J.: Gas-phase ion-molecule reactions using regioselectively generated radical cations to model oxidative damage and probe radical sites in peptides. Org. Biomol. Chem. **9**, 3733–3745 (2011)
70. Dechamps, N., Flammang, R., Boulvin, M., Lamote, L., Gerbaux, P., Ngan, V.T., Nguyen, M.T.: Ion-molecule reactions involving methyl isocyanide and methyl cyanide. Eur. J. Mass. Spectrom. **13**, 385–395 (2007)
71. Holm, A.I.S., Hvelplund, P., Kadhane, U., Larsen, M.K., Liu, B., Nielsen, S.B., Panja, S., Pedersen, J.M., Skrydstrup, T., Stochkel, K., Williams, E.R., Worm, E.S.: On the mechanism of electron-capture-induced dissociation of peptide dications from ^{15}N-labeling and crown-ether complexation. J. Phys. Chem. A **111**, 9641–9643 (2007)
72. Moss, C.L., Liang, W., Li, X., Tureček, F.: The early life of a peptide cation radical. Ground and excited-state trajectories of electron-based peptide dissociations during the first 330 femtoseconds. J. Am. Soc. Mass Spectrom. **23**, 446–459 (2012)
73. Syrstad, E.A., Tureček, F.: Toward a general mechanism of electron-capture dissociation. J. Am. Soc. Mass Spectrom. **16**, 208–224 (2005)
74. Sobczyk, M., Anusiewicz, I., Berdys-Kochanska, J., Sawicka, A., Skurski, P., Simons, J.: Coulomb-assisted dissociative electron attachment: application to a model peptide. J. Phys. Chem. A **109**, 250–258 (2005)
75. Hayakawa, S., Hashimoto, M., Matsubara, H., Tureček, F.: Dissecting the proline effect: dissociations of proline radicals formed by electron transfer to protonated Pro-Gly and Gly-Pro dipeptides in the gas phase. J. Am. Chem. Soc. **129**, 7936–7949 (2007)